



## Anton de Kom Universiteit van Suriname Bibliotheek

Universiteitscomplex, Leysweg 86, Paramaribo, Suriname, Postbus 9212  
Telefoon (597)464547, Fax (597)434211, E-mail: [adekbib@uvs.edu](mailto:adekbib@uvs.edu)

### APPROVAL

NAAM: ..... *Anuradha Monorath* .....

verleent wel / niet aan de AdeKUS kosteloos de niet-exclusieve toestemming om haar / zijn Drs. / B.Sc. / M.Sc.  
afstudeerscriptie online beschikbaar te stellen aan gebruikers binnen en buiten de AdeKUS.

Plaats en datum, ..... *14 Augustus 2019* .....

Handtekening ..... *[Signature]* .....



**Anton de Kom University of Suriname**

**Faculty of Technology**

Academic year: 2018-2019

***Analysis and modeling of land use and land cover  
change in the Tapanahony River basin***

by

ANURADHA MONORATH

A thesis submitted to the Anton de Kom University of Suriname, Faculty of Technology, Suriname, in fulfillment of the requirements for the degree of Master of Science (MSc) in Sustainable Management of Natural Resources

**Supervisor:**

*R. Nurmohamed Ph.D.*

**Date:** July 3, 2019

Paramaribo, Suriname

## **Preface**

Always being impressed by the work of NASA (National Aeronautics and Space Administration), made my search for a thesis topic of interest, easier during my Master of Science study period. This particular subject got my attention because of its focus on land use modeling, spatial planning, the interpretation of satellite images and the application of remote sensing that contributes to the sustainable management of natural resources. My gratitude goes to the Belgian Directorate-General for Development Cooperation (DGDC) and the Flemish Interuniversity Council (VLIR-UOS) for making the Master of Science Program in Sustainable Management of Natural Resources (MSc in SMNR) possible at the Anton de Kom University of Suriname. I would also like to express the deepest appreciation to my supervisor and guide Dr. Riad Nurmohamed and Ms. Kimberly Fung-Loy MSc., without whom this thesis would not have proceeded to completion. Their input, guidance and persistent help has been valuable in ensuring this thesis is of the highest quality. Special thanks goes further to those who have made much effort in supporting me with seeking data, literature and providing me with valuable feedback. Within this regard I am hereby thankful to the following persons; Ms. Sarah Crabbe MSc. and her team from the Forest Cover and Monitoring Unit of the SBB, the Staff of NARENA and the staff employees from the GMD of the Ministry of Natural Resources for providing the data, as well as their valuable input towards what the data contained and how it was produced, thus immensely reducing the time and effort that would have been required to collect data. I'm grateful to the Permanent Secretary of the Ministry of Natural Resources Mr. Drs. Dave Abeleven for the time and opportunity given to me to attend and finish the SMNR program. Finally, I would like to tribute and acknowledge with gratitude, the endless support and love of my beautiful family and my great father and dear mother. They all kept me going, and this thesis would not have been possible without them. I will cherish this graduate experience definitely forever.

## List of figures

Figure 1: Overview of the study area	10
Figure 2: DEM of the study area (Projected)	16
Figure 3: Image mosaicking	18
Figure 4: Signature comparison chart of clouds and cloud shadows with different LULC classes	19
Figure 5: Comparison of the signatures of the LULC classes for the Tapanahony- River basin	21
Figure 6: Random sampled points used for accuracy assessment	24
Figure 7: Gold exploration layers along the Toso and the Sela creek	27
Figure 8: Possible driver variables modeled as distance map	28
Figure 9: The primary (proposed), secondary and tertiary roads within the study area	32
Figure 10: Steps in the flowchart to address the LULC analysis and prediction process	34
Figure 11: The classified LULC map of the year 2004 and 2014	35
Figure 12: Gains and losses occurring between 2004 and 2014 in the Tapanahony River basin	37
Figure 13: Net change in km <sup>2</sup> in the Tapanahony River basin between 2004-2014	37
Figure 14: Contributors to net change in Cropland & grassland (km <sup>2</sup> )	37
Figure 15: Contributors to net change in Built-up land (km <sup>2</sup> )	38
Figure 16: Contributors to net change in Mines (km <sup>2</sup> )	38
Figure 17: LULC Surface Area by Category	39
Figure 18: Transition Potential Map: Forest to Cropland and Grassland	41
Figure 19: Transition Potential Map: Forest to Mines	42
Figure 20: Transition Potential Map: Forest to Built-up land	43
Figure 21: Comparison of the LULC map of reality Hansen_GFC-2016-v1.4_last_10N_060W1 vs. Predicted land cover map of 2016	43
Figure 22: The trend of classes changing in area size (km <sup>2</sup> ) for scenario 1	46
Figure 23: The trend of classes changing in area size (km <sup>2</sup> ) for scenario 2	46
Figure 24: Hard predicted LULC maps of the years 2020, 2030 and 2040 under scenario 1 and scenario 2	48
Figure 25: Soft predicted LULC maps of the years 2020, 2030 and 2040 under scenario 1 and scenario 2	49

## List of tables

Table 1: Specifications of Landsat 5 TM bands (Lillesand, 2015)	13
Table 2: Characteristics of the Landsat – 8 Spectral Bands (Lillesand, 2015)	13
Table 3: Main images of the year 2004 and 2014, with the lowest scene cloud cover selected for image classification	14
Table 4: Supplementary Landsat images used for gap filling	14
Table 5: Landsat 5 and Landsat 8 equivalent bands	16
Table 6: LULC classes and description based on Anderson classification scheme	20
Table 7: Possible driver variables	27
Table 8: Error matrix for the landsat 2014 classification map	35
Table 9: Overview of the accuracies and KIA's	36
Table 10: Changes occurring between 2004 and 2014 in the Tapanahony River basin	36
Table 11: Amount of area changed per transition	39
Table 12: Driver variables tested with the Cramer V	40
Table 13: Accuracy, skill and driver assessment of the Sub-model Forest to Cropland and Grassland	41
Table 14: Accuracy, skill and driver assessment of the Sub-model Forest to Mines	42
Table 15: Accuracy, skill and driver assessment of the Sub-model Forest to Built-up land	43
Table 16: Error Matrix for the Predicted LULC map of 2016	45
Table 17: Changes in areas of LULC classes of interest under scenario 1 for the year 2014, 2020, 2030 and 2040	47
Table 18: Changes in areas of LULC classes of interest under scenario 2 for the year 2014, 2020, 2030 and 2040	47

## List of abbreviations

ASGM	Artisanal and Small –Scale Gold Mining
CA	Cellular Automata
CELOS	Centre for Agricultural Research in Suriname
DEM	Digital Elevation Model
DN	Digital Number
GIS	Geographic Information System
GMTED	Global Multi-resolution Terrain Elevation Data
GMD	Geology and Mining Department
FAO	Food and Agricultural Organization of the United Nations
FLDA	Fisher Linear Discriminant Analysis
HFLD	High Forest Cover, Low Deforestation
KIA	Kappa Index of Agreement
LCM	Land Change Modeler
LULC	Land Use and Land Cover
L1TP	Standard Terrain Correction
MLP	Multi-Layer Perceptron
NTFP	Non Timber Forest Products
NIR	Near Infra Red
SWIR	Short-Wavelength Infra Red
OLI	Operational Land Imager
REDD+	Reducing Emissions from Deforestation & Forest Degradation +
SBB	Foundation for Forest Management and Production Control
SRTM	Shuttle Radar Topography Mission
TM	Thematic Mapper
TIRS	Thermal Infrared Sensor
UNFCCC	United Nations Framework Convention on Climate Change
USGS	United States Geological Survey
UTM	Universal Transverse Mercator
WGS	World Geodetic Systems

## Table of contents

Preface.....	i
List of figures.....	ii
List of tables.....	iii
List of abbreviations.....	iv
Executive Summary.....	1
1. Introduction.....	2
1.1. Problem description.....	3
1.2. Research Objectives.....	3
1.3. Research questions.....	4
1.4. Outline thesis.....	4
2. Literature review.....	5
2.1. Remote sense imagery and LULC classes .....	5
2.2. Image classification.....	5
2.3. Drivers of LULC change .....	7
2.4. LULC change modeling and software.....	7
2.5. Previous and recent LULC change studies in Suriname.....	9
3. Methodology.....	10
3.1. The study area.....	10
3.2. Materials.....	12
3.3. Image enhancement of landsat images.....	15
3.3.1 Image restoration.....	17
3.3.2 Cloud and cloud shadow masking.....	18
3.4. Image classification.....	19
3.5. Accuracy Assessment.....	23

3.6. Past LULC change analysis between 2004-2014.....	25
3.6.1 Driver variables.....	25
3.6.2 LULC transition modeling.....	28
3.7 Model comparison and validation.....	30
3.8 Change Prediction maps.....	31
3.8.1 Change Prediction Process.....	31
3.8.2 Proposed road intervention.....	33
4. Results.....	34
4.1. Image classification.....	34
4.2. Accuracy assessment.....	35
4.3. Past LULC analysis between 2004-2014.....	36
4.4. Transition potential modeling.....	39
4.4.1 Driver testing.....	39
4.4.2 Transition sub-model ‘Forest to Cropland and Grassland’ .....	40
4.4.3 Transition sub-model ‘Forest to Mining’.....	41
4.4.4 Transition sub-model ‘Forest to Built-up land’.....	42
4.5. Model comparison and validation.....	44
4.6. Change Prediction.....	45
5. Discussion.....	50
6. Conclusions and recommendations.....	52
6.1. Conclusions.....	52
6.2 Recommendations.....	53
References.....	55
Appendices.....	i
Appendix 1. USGS land use and land cover classification system.....	i
Appendix 2. Indicative Classification Map of the Republic of Suriname.....	ii
Appendix 3. Error matrix for the landsat 2014 classification map.....	iii

## **Executive summary**

Human induced changes in land cover may result in deforestation that in turn may lead to unsustainable changes in the land use and land cover. The presence of forest is of importance for ecosystem services. If threats to the ecosystem services are left unattended, the environment will continue to deteriorate. In order to prevent this, the drivers of deforestation needs to be addressed, understood and measured to create policies, incentives, and systems for sustainable development and forest conservation. This study aims to analyze and model land uses and land cover between 2004 and 2014 in the Tapanahony River basin and to predict future changes, using Landsat images and the Idrisi Land Change Modeler. The changes of interest were the transitions from the land use and land cover classes 'Forest' to 'Cropland and Grassland', 'Built-up land' and 'Mines'. For the changes occurring between 2004 and 2014, transition potential models were created with driving variables to explain the changes. These models were then used to project the future land use and land cover. These future projections were for the business as usual scenario and the Tapajai project scenario, indicating proposed roads. Results showed that between 2004 and 2014 the major changes occurring in the study area were the transitions from 'Forest' to 'Cropland and Grassland', followed by changes in the transition from 'Forest' to 'Mines' and the transition from 'Forest' to 'Built-up land'. With reference to the trend between 2004 and 2014, future projections for the years 2020, 2030 and 2040 showed that deforestation will proceed into the future. The Tapanahony River basin has no proper road establishment and is sparsely populated by indigenous and tribal people communities. Expected population growth, government planning interventions and the growing demand of gold exploitation will be mainly at the expense of deforestation and the ecosystem integrity of remaining forest in the future. Multidisciplinary studies will be required to access the implications of these expected LULC changes.

**Keywords:** Suriname, land-use and land- cover change, drivers of forest change, Land Change Modeler, planning interventions, infrastructure, simulation of deforestation.

## **1. Introduction**

Population statistics from the General Statistical Office in Suriname, show a growth in population of 14% from 2005 to 2015 (Algemeen Bureau voor de Statistiek in Suriname, 2015). The needs and wants of a growing population often lead to an increased use of natural resources by for example agriculture expansion, wood extraction, mining, energy need, infrastructure expansion such as road building and urbanization. Forests provide a multitude of environmental, economic and social benefits. People obtain benefits from ecosystems services, including income and food security for local communities (Foley, J.A., et al.2005, FAO, 2015). Countries gain national income from the forest such as the export of wood and global environmental benefits by forest climate mitigation for carbon sequestration (Favero, A., et.al, 2018, FAO, 2015). An increasing deforestation can lead to the degradation of ecosystem services that in turn can cause significant harm to the human well-being. The growing demand on natural resources leads to unsustainable land use and land cover changes. These unsustainable changes can result in deforestation, meaning the long-term or permanent loss of forest cover and implies transformation into another land use or land cover type (FAO, 2007). Direct drivers of deforestation and forest degradation are human activities and actions that directly impact forest cover and result in loss of carbon stocks (Kissinger, 2012). Considering the above, it is critical to monitor past land use and land cover (LULC) changes and to study the drivers of deforestation. This is done through land use planning by first analyzing data from past deforestation through LULC change detection analysis that can be further realized by a land use modeling approach. Land use models are capable of exploring the transition potentials of various LULC types for a given set of driver variables (Kamusoko, 2009). The information can then be used for predicting future LULC information. The use of spatial modeling to predict the location of future deforestation may serve to provide information on where the greatest deforestation pressures may be, necessary for the government authorities or policymakers to use such inputs to make land -use planning decisions or constrain to sustainable levels and to provide better management of land use and land cover.

## **1.1 Problem description**

Fonseca et al. (2007) identified that countries with more than 50% forest cover and a deforestation rate below 0.22% per year are considered to fall into the High Forest cover and Low rates of Deforestation (HFLD) category, based on their remaining forest cover and deforestation rate. With more than 14.8 million ha of forest cover (93% of its total area), Suriname is one of the most forested countries in the world. Historical annual rates of deforestation below 0.1%, have allowed the country to be classified as a HFLD country (SBB, 2018, Unique, 2017). Surinamese forests provides a multitude of environmental and social benefits, including income and food security for local communities, national income from logging and mining, and global environmental benefits such as climate mitigation and biodiversity preservation. Suriname's forests act as a carbon sink, making it a carbon-negative country (Unique, 2017). Changes in these services affect human well-being through impacts on security, the necessary material for a good life, health, and social and cultural relations (Millennium Ecosystem Assessment, 2005). While the forests in Suriname have a long history of being relatively undisturbed, it cannot be assumed that it will persist in the future. Drivers and pressures on Suriname's forests, in other words the underlying and direct causes of deforestation and forest degradation, are becoming increasingly pertinent since the country has entered a new era of economic and industrial development (Unique, 2017). In order to keep the country's HFLD status to safeguard the protection of the ecosystem services and to ensure a healthy living environment for citizens, it is important to monitor current deforestation trends, predict future deforestation expansion for measures to be taken timely to control and guide the drivers of deforestation.

## **1.2 Research objectives**

In this study a time period of 2004-2014 is used, while FAO (FAO, 2010 a) reports uses time periods of 2000-2005 and 2005-2010. This study period was chosen, due to the lack of cloud-free images available for the year 2005 and 2015.

This thesis study aims to capture the LULC change in the Tapanahony River Basin to compare scenarios using remote sensing, GIS and modeling techniques. For the comparison of future LULC trends, two scenarios are applied:

- 1) the business as usual scenario, where the future LULC changes are predicted on the assumption that operating conditions or applied policies remain what they are at present.
- 2) the examination of forest areas at risk of being deforested by the constructions of new roads from the proposed Tapajai hydropower project. This project is chosen as a second scenario, because its implementation is mentioned in the national policy development plan 2017-2021 of Suriname.

The specific objectives encompassed by this study are:

- to analyze the changes in land use and land cover between 2004-2014, occurring within the Tapanahony River Basin, based on the analysis of remotely sensed satellite imagery,
- to model the transition potentials for each LULC type of interest by identifying and incorporating explanatory variables or drivers that drive or explain changes of deforestation.
- to predict future LULC scenarios for the years 2020, 2030 and 2040.

### **1.3 Research questions**

The research questions of this thesis are:

- What were the LULC changes across the period 2004 - 2014?
- What will be the expected LULC changes in the Tapanahony River basin across the years 2020, 2030 and 2040 under the business as usual scenario?
- What will be the expected LULC changes in the Tapanahony River Basin across the years 2020, 2030 and 2040 under the Tapajai project?

### **1.4 Outline thesis**

This study starts with a general description of the problem in chapter one, which is further narrowed down to the specific description, specific research objectives and research questions. Literature review with regards to LULC change analysis, modeling and classification is presented in chapter two. The methodology used to meet the objective and answering the research questions in particular is described in chapter three. This consists of image classification, change analysis, transition modeling and change prediction. The results are presented in chapter four and are discussed in chapter five. Finally the conclusions and recommendations are respectively presented in chapter six.

## **2. Literature Review**

### **2.1 Remote sense imagery and LULC classes**

Timely and accurate gathering of information on the changes of land use and land cover of an area supports the analysis of LULC change. LULC change analysis is important for many planning and management activities and is considered an essential element for modeling and understanding the earth as a system (Lillesand, et al., 2015). For the LULC change analysis, remotely sensed data of the study area is used for land cover and land use categories to be mapped by a classification system (Anderson, 1976). The U.S. Geological Survey (USGS) developed one of the first LULC classifications systems for the use with remotely sensed imagery of which the basic concepts are still valid today. The Anderson LULC Classification system (Appendix 1) is designed to use four (4) levels of classification, consisting of land cover categories and subcategories (Lillesand, et al., 2015). Level I and Level II classes are defined by the USGS. Level I is designed to be used with low to moderate resolution of 20 to 100 m satellite data e.g., Landsat MSS data and consist of nine level I classes, which account for 100% of earth's surface. Level II classification requires a representative format for image interpretation from small-scale aerial photographs with moderate resolution of 5 to 20 m. Several level II categories (and in some instances, level III categories) have been interpreted from landsat 30 m resolution data. Level III requires large amounts of supplementary information in addition to large scale areal images of 1- 5 m (e.g. IKONOS). Level IV requires large-scale aerial photographs or high resolution satellite data (e.g., Quickbird data) with a resolution of 0.25 to 1 m. (lillesand, et al., 2015). Several land use/land cover mapping efforts have been undertaken worldwide to use the USGS land use/land cover classification system, or variations thereof. In this study a classification of level II was done for analyzing LULC changes using Landsat 5 and Landsat 8 images. A combination of Landsat 5 Thematic Mapper (TM) and Landsat 8 Operational land Imager (OLI) data have been used in many studies of LULC change (Sharma, et al., 2017, Coulter, et al., 2016; Leh, et al., 2013; Zhang, et al., 2014; Regmi, et al., 2014).

### **2.2 Image Classification**

Image classification procedures is to automatically categorize all pixels in an image into land cover classes or themes. There are four (4) classification procedures identified by Lillesand et al., (2015): 1) Spectral pattern recognition, 2) Spatial pattern recognition, 3) Temporal pattern recognition, and 4) Object-oriented classification. Spatial pattern classifiers attempt to mimic

spatial synthesis in the visual image interpretation process. This technique is much more complex and thus more computationally intensive than spectral recognition procedure, which automated classification is based on pixel-by-pixel spectral information (spectral signature). Object-oriented classification procedures are more computationally intensive and generally achieve higher accuracy (Lillesand et al., 2015). Software packages as IDRISI and ARCGIS offer both image classification techniques from multispectral satellite images. Spectral pattern recognition have historically formed the basis of multispectral classification and consist of two (2) types of classification methods:

1. Supervised: this technique involves the collection of training samples where the user identifies regions in the image by delineating polygons, known as training sites to derive spectral signatures of pixels in an image in order to distinguish between different classes. The classification algorithm then classifies each pixel in the rest of the image based on comparisons with training data, to determine which class each pixel belongs to (Warner, 2013). Supervised classification is an approach that is commonly used for remotely-sensed data classification (Hubert-Moy et al., 2001; Lu & Weng, 2007), and requires a sufficient number of training samples to perform a successful classification (Campbell, 2006; Myburgh & Van Niekerk, 2013, Warner, 2013).

2. Unsupervised: this technique involves no training samples. The algorithm identifies the spectral classes and then the user assigns an informational utility to each class (Eastman, 2012).

A supervised classification is recommended when the user is interested in a particular class, possibly consisting of multiple spectral classes. In this case it is important to delineate a sufficient number of training pixels in the training sites. The higher the number of pixels the better the statistical representation of the class. A general rule of thumb is that the number of pixels in each training set should not be less than 10 times the number of spectral bands (Warner, 2013). Hereafter a statistical based classifier is utilized to determine the class pixel. There are two types of classifiers: 1) soft classifier and 2) hard classifier. The soft classifier offers a map in which the probabilities of the pixels belonging to each class is recorded. A hard classifier makes a decision to which class such pixel belongs, based on the highest probability (Eastman, 2012). Various mathematical algorithms such as the Fisher linear discriminant analysis, Minimum distance to mean and the Maximum likelihood are available, producing hard and soft classified images (Eastman, 2012, Lillesand et al. 2015).

### **2.3 Drivers of LULC change**

The dynamics of deforestation depends on a variability of actors that needs to be assessed in forested areas. A distinction is commonly made between proximate/direct causes and underlying/indirect causes of deforestation and forest degradation. Proximate or direct drivers of deforestation and forest degradation are human activities and actions that directly impact forest cover and result in the loss of carbon stocks such as shifting cultivation, wood extraction, settlement expansion, infrastructure extension and mineral extraction (Geist and Lambin, 2002). Underpinning these proximate causes are underlying causes, a complex of economic issues, policies, cultural or sociopolitical concerns, governance and demographic factors (Kissinger, 2012). Underlying and direct drivers of deforestation are becoming increasingly pertinent since the country has entered a new era of economic and industrial development, therefore it is often important to address them separately and examine them at various scales for specific analysis and intervention strategies.

### **2.4 LULC change modeling and software**

LULC change can be described and projected through Land change models (LCMs). Land change models are powerful software program tools that can be used to visualize and analyze the causes of LULC change. At the request of the USGS and NASA, the National Research Council established a committee to describe various LCM approaches, suggest guidance for their appropriate application, and describe ways to improve the integration of observation strategies into the models. A wide variety of LCMs has been developed to examine land change processes to make land use and land cover predictions. The committee grouped six categories of modeling approaches arranged in order from least to most focus on the process: 1.) Machine learning and statistical, 2) cellular, 3) sector-based economic, 4) spatially disaggregate economic, 5) agent based and 6) hybrid. The best modeling approach to use, depends on the application. The relative advantages of the approaches for particular purposes can be used in various policy and decision-making context. The approaches that rely on data about land-change patterns, including Machine Learning and Statistical, and Cellular, tend to use land-cover information from satellite imagery, and relationships based on observed changes in the past. These approaches are easy to implement, are useful for projecting observed land-cover changes over short periods into the future, and they can provide valuable descriptions and projections of patterns and trends. The more process-based approaches, such as Sector-Based Economic, Spatially Disaggregate Economic, and Agent-Based models, make

greater use of social science information about land-change processes. These latter approaches provide more realistic representations of the processes of change and include social aspects such as policy implementations, but they are more complex and therefore more difficult to calibrate and validate than the machine learning and cellular models. A hybrid model combines aspects of the previous types of models into a new single model (Committee on Needs and Research Requirements for Land Change Modeling; Geographical Sciences Committee; Board on Earth Sciences and Resources; Division on Earth and Life Studies, 2013). Most models utilize some version of Cellular Automata (CA) where cells in a grid change state are based on a set of rules considering the states of the neighboring cells of which all cells only have a certain set of discrete states. These cellular models have widely been used in modeling spatial problems in particular LULC studies (He et al, 2006). The complexity of Cellular increases when more LULC classes are applied or incorporated due to the presence of more dynamic spatial variables and transition possibilities. The added complexity of this model is taken care of, by incorporating multi-layer perception neural networks to model transition potentials of various LULC types. These neural networks have the advantage of capturing non-linear features and they are more resilient to handle incorrect and poor data (Li & Yeh, 2002). There are many approaches and software packages for modelling LULC and many of them are based on past LULC such as CLUE-S (Conversion of Land Use and Its Effects at Small regional extent), DINAMICA EGO, CA\_MARKOV and Land Change Modeler (Mas, et al., 2012; Mas, 2014; Han, et al.,2015). Each LULC model has its own advantages and shortcomings. Software packages for LULC modeling such as DINAMICA EGO (Soares-Filho et al., 2002) and Land Change modeler (Eastman, 2012) were initially developed for monitoring and mapping deforestation. Both modelers require no knowledge beforehand as compared to CLUE-S. Their modeling approaches are based on the simulation of land use spatial patterns. By comparing the LULC of two map trends, driver variables are automatically tested and mapped spatially after which areas with the transition potential to undergo change, are mapped. A third classified image is then used to validate the model, making multiple LULC scenarios possible in order to predict future land use demand (He et al, 2006). DINAMICA EGO offers more realistic prospective maps with respect to landscape pattern, by simulating changes in areas with lower change potential, because of its sophisticated modeling approach. The user builds the entire land change model using multiple sub models (Mas, et al., 2012, Mas, 2014). CA\_MARKOV, CLUE, and LCM on the other hand are limited to areas with higher change potential. LCM has a rigid structure, as there are no possibilities to modify the internal processing of the model for allocating change. Besides

of LCM having a rigid structure, it also has a less complex structure and is therefore beneficial to use when little proficiency in the use of LCM is present (Mas, et al., 2012, Soares-Filho et al., 2002). In this research, the LCM of the Idrisi software will be used for LULC change analysis. The LCM has been used to study LULC changes and to predict future deforestation in Suriname (Fung-Loy, 2014, Crema et al., 2014). It was also used in different other countries as China (Zhang et al., 2010), USA (Chicago) (Wilson et al., 2011) and India (Jain et al., 2013). The Idrisi software is licensed and was familiar to work with, since it was practiced during the course of Remote Sensing of the VLIR-AdekUS MSc program. Idrisi incorporates CA Markov in its LCM package and models the potential for change using past land transition information and includes explanatory variable maps that might drive or explain such change. Variables can be tested to confirm whether or not they hold explanatory power for the transition. LCM can create or model land cover transition potential that express the likelihood that a land will transition in the future. Each transition can be modeled with either logistic regression, SimWeight a modified machine- learning procedure and a Multi-Layer Perceptron (MLP) neural network, resulting in a potential map for each transition (an expression of time-specific potential for change) with full reporting on the explanatory power of driver variables, used for the prediction of future LULC in the study area.

## **2.5 Previous and recent LULC change studies in Suriname**

Several studies has been previously and recently performed on the analysis of LULC changes in Suriname. In 2010 a case study was done to model the effects of new road infrastructure on land use change, from 2011 until 2025, using the Clue Scanner (van Dijck, et al., 2013). In 2011 Sarah Ramirez-Gomez analyzed the deforestation of an area located in eastern Suriname between 2005 and 2009, and predicted future deforestation for 2020 using the DINAMICA EGO software version 1.6.2. (Ramirez-Gomez, S., 2011). A study for the entire of Suriname was done in 2012, within the framework of an ACTO (Amazon Cooperation Treaty Organization) project named Monitoring Deforestation, Logging and Land Use Change in the Pan Amazonian Forest. The Forest Cover Monitoring Unit (FCMU) of The Foundation for Forest Management and Production Control (SBB) was in charge of this project, using Landsat images and the Terra Amazon software, a freeware distributed by the Brazilian Institute for Space Research (INPE). Within the framework of developing a land use change model for the Suriname National Redd+ (Reducing Emissions from Deforestation & Forest Degradation) strategy plan, the deforestation in Suriname was simulated using DINAMICA EGO in 2017

(Crabbe et al., 2012). Stefano Crema of the Clark Labs executed a regional scenario modeling project for the Guiana Shield, in close collaboration with Conservation International with the purpose to analyze LULC changes and to model future deforestation trends with the Idrisi Land Change Modeler (Crema, S., 2014)

### 3. Methodology

#### 3.1 The study area

The Tapanahony River basin is situated in the district Sipaliwini in the South Eastern part of Suriname. It covers an area which is situated approximately between 2.25° and 4.25° N.L. and 54.50° and 56.25° W.L., has a total drainage area of about 19,715 km<sup>2</sup>. Based on the topography that varies from 39 m to 911 m above mean sea level, the study area can be divided in a low-lying terrain in the northern region and a high-lying terrain in the southern region. The mean elevation is about 239 m. (Nurmohamed et al., 2013). The Tapanahony River basin is represented in Figure 1, by the red color with its rivers depicted in dark blue.

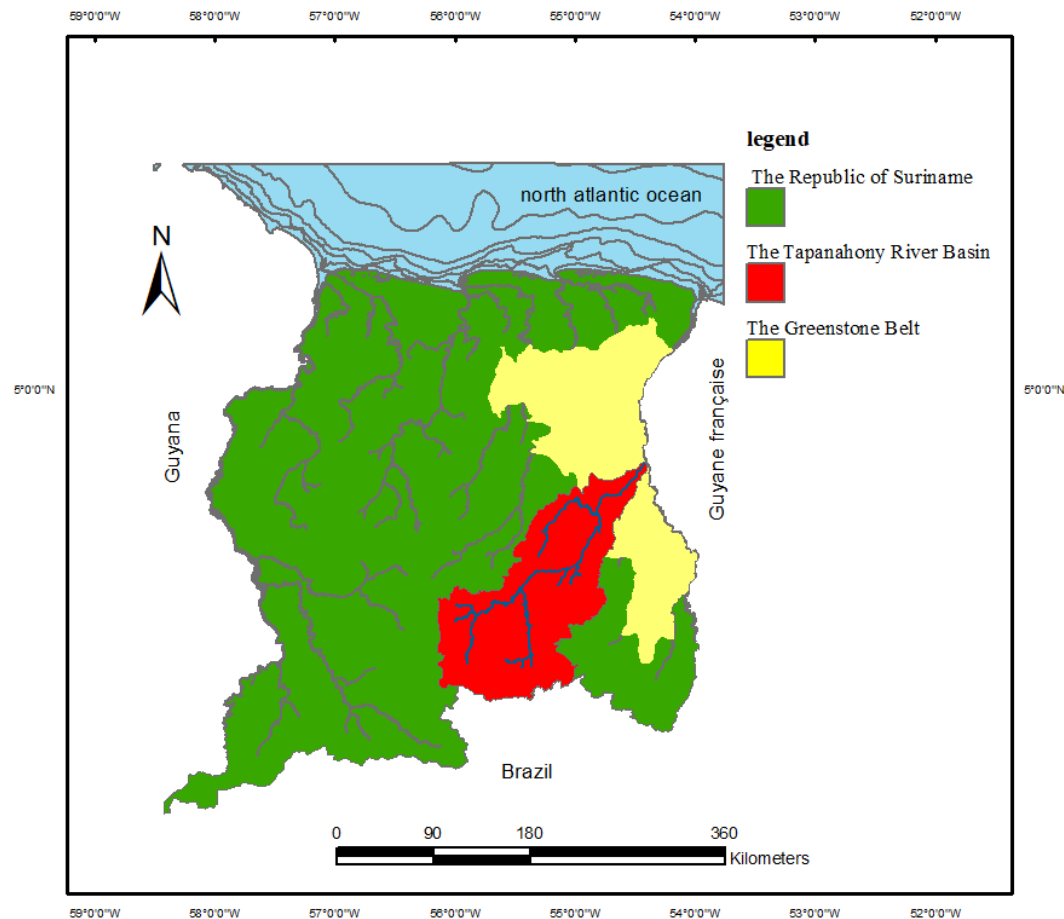


**Figure 1.** Overview of the study area

The Tapanahony River is a major river in the south eastern part of Suriname. The river originates in the Southern part of the Eilerts de Haan Mountain, near the border with Brazil. It joins the Marowijne River at a village called Stoelmanseiland. The area has an extensive network of navigable creeks, which provide drainage and supply water to both people and wildlife (Nurmohamed et al., 2013). The villages within the Tapanahony River basin are mostly located along the river banks for more convenience, as the waterways are the main transport routes (apart from some airstrips) and water of the rivers is used for household purposes (cooking, washing, bathing, drinking etc.). The population is comprised by Maroon and Indigenous communities. The Jai creek basin is not inhabited, though some gold mining camps are located between the Jai creek and the Toso creek. The communities along the Lower-Tapanahoni River consist of the Aucaner Maroon (Ndyuka) Nation, descendants of the escaped slaves who settled in the region during the 18th century. There are about 5,000 Aucaners Maroons living in 26 villages on the lower portion of the Tapanahoni River. Many of these villages are located on islands in the river. These villages vary in size from a few families to villages of over 500 persons (Drietabiki). The villages of the Godo Olo cluster have over 1,000 inhabitants. Members of the Wayana Indigenous Nation inhabit the middle portion of the Upper Tapanahony River and live in the village of Apetina (also called Peleowime). This village has about 350 inhabitants. Members of the Trio Indigenous Nation inhabit the upper portion of the Tapanahoni River. Some 500 Trio persons live in the village of Pelelu Tepu (refer as Tepu). About 250 persons live in the village of Palumeu, just downstream from Tepu, which consists of both Wayana and Trio inhabitants (Staatsolie N.V., 2013). For the Trio, Wayana and Maroon communities the rainforest is their place of both residence and survival. The forest is a complex of ecosystems which they have used for their survival and sustained for centuries and even millennia. Traditionally the indigenous as well as the Maroon communities are living from shifting cultivation agriculture, hunting, fishing and gathering. Local communities depend on the forest area mainly for food security in terms of crops, fruit and game, and practice fishing in the rivers. The forest is burnt during shifting cultivation and the land is being prepared for agriculture purposes where after it is left abandoned and overgrown with secondary forest vegetation. Traditionally they abandon the areas they plant, hunt and fish, and moved to a new location. Eco-tourism is increasing in some of the villages of the tribal communities where airstrips are located and where the villagers offer boat transport services with their own canoes with outboard motors. A very wide range of non-timber forest products (NTFPs) is collected as required or when available used and sold by tribal

communities. Wood is used mainly for boats and construction of houses or other smaller projects. (Noordam, et.al, 2007, Heemskerk, et. al., 2007). Most important land uses consist of gold mining which is closely associated with the distribution of the green stone belt, abandoned plantation and shifting cultivation. The northern section of the study area intersects with the Greenstone belt, the geological formation where gold mining takes place. The Greenstone belt is an area of 24,000 km<sup>2</sup> which contains most of the gold deposits in Suriname and runs from the south-eastern corner of Suriname to the northwestern area around the Goliath Mountain. There are many small-scale gold mining activities within that part of the area that overlaps with the Greenstone belt. Small-scale gold mining is taking place in parts of the Ndyuka territory and is the main source of income for most of the local Maroons inhabitants living in the basin. A small amount of small scale miners are active in the Sela and Toso creeks within the Tapanahony River basin, situated both in the Greenstone-belt where forest is cut and cleared, in preparation for the alluvial gold mining practices. In alluvial mining, gold is extracted from channels, lakes or creeks where fine gold particles have gathered at the bottom of the water body and formed a mineral deposit. When a mine is depleted, the miners move to another area, leaving behind areas of bare soil and water filled mines (Heemskerk, 2000). Gold operation are facilitated by easy transportation possibilities over waterways or human induced unpaved roads. The end section of the thirty-year-old, 92 km long secondary road from Pokigron to Jaikreek is also situated in the area, and was rehabilitated in 2010 by the state oil company “Staatsolie Ltd”.

### **3.2 Materials**

For the prediction of future LULC, land cover maps are necessary for the LCM to use. The images used for the creation of the land cover maps were downloaded from the USGS website using the publicly available geological survey Earthexplorer website (USGS, Earthexplorer, 2018a). For this study, Landsat Thematic Mapper at a resolution of 30 m of the year 2004 was used for land use/cover classification. Since the TM sensor began its decommissioning activities in January 2013, images from Landsat 8 satellite sensor OLI and TIRS were downloaded for the year 2014. Landsat 8 has enhanced capabilities including new spectral bands, two thermal bands, improved sensor signal-to-noise performance and associated improvements in radiometric resolution (Roy et al., 2014). Landsat 7 images were not applied in this study because the system’s Scan Line Corrector (SCL) failed on May 31, 2003, containing data gaps and duplications (Lillesand, 2015). Both Landsat 8 and 5 Landsat images

belonging to the collection category T1, were selected with less scene cloud cover. The images were orthorectified with precision terrain correction level L1TP by the USGS. Level T1 images are terrain and geometrically corrected, they guarantee systematic radiometric and topographic accuracy by using ground control points. The level 1 images are available for download at no charge and are generated using the UTM-21 N reference system (Engebretson C., 2018.). The detailed specifications of data are presented in Table 1 and Table 2.

**Table 1.** Specifications of Landsat 5 TM bands (Lillesand, 2015)

<b>Band</b>	<b>Band Width (<math>\mu\text{m}</math>)</b>	<b>Spatial Resolution (m)</b>	<b>Sensor</b>
Band 1 - Blue	0.45 – 0.52	30	TM
Band 2 - Green	0.52 – 0.60	30	TM
Band 3 - Red	0.63- 0.69	30	TM
Band 4 -Near Infrared	0.76 – 0.90	30	TM
Band 5 - Short-wave Infrared	1.55 – 1.75	30	TM
Band 6 -Thermal Infrared	10.40 – 12.50	120	TM
Band 7 - Short – wave Infrared	2.08 – 2.35	30	TM

Several of the Landsat- 8 reflective bands provide sufficient data consistency with landsat 5 in terms of acquisition geometry, coverage, spectral and spatial characteristics, calibration, output data quality, and data availability to permit assessment of LULC. However the widths of several of the OLI bands are refined and narrow in order to lessen the influence of various atmospheric absorption features (Lillesand, 2015, Roy et al., 2014).

**Table 2.** Characteristics of the Landsat – 8 Spectral Bands (Lillesand, 2015)

<b>Band</b>	<b>Band Width (<math>\mu\text{m}</math>)</b>	<b>Spatial Resolution (m)</b>	<b>Sensor</b>
Band 1- Coastal/Aerosol	0.433-0.453	30	OLI
Band 2 - Blue	0.450-0.515	30	OLI
Band 3 - Green	0.525-0.600	30	OLI
Band 4 – Red	0.630-0.680	30	OLI
Band 5 – Near Infrared	0.845-0.855	30	OLI
Band 6 - Short-wave Infrared	1.560-1.660	30	OLI
Band 7- Short – wave Infrared	2.100-2.300	30	OLI
Band 8- Panchromatic	0.500-0.680	15	OLI
Band 9- Cirrus	1.360-1.390	30	OLI
Band 10- TIR 1	10.6-11.2	100	TIRS
Band 11- TIR 2	11.5-12.5	100	TIRS

The study area was covered by four Landsat images. Eight main images were downloaded from the USGS website for the years 2004 and 2014, according to the Worldwide Reference System 2- (WRS-2) path/row system (Table 3). These images had the least scene cloud cover. Parts of useful images from the years 2004, 2005 and 2015 that were partially cloud free are presented in Table 4 and were used for filling gaps in the main images, which were created by cloud masking.

**Table 3.** Main landsat images of the year 2004 and 2014, with the lowest scene cloud cover selected for image classification

<b>Year</b> <b>Path/Row</b>	<b>2004</b>	<b>2014</b>
<b>228/57</b>	LT52280572004315CUB00	LC82280572014246LGN01
<b>228/58</b>	LT52280582004315CUB00	LC82280582014246LGN01
<b>229/57</b>	LT52290572004338CUB01	LC82290572014301LGN01
<b>229/58</b>	LT52290582004322CUB00	LC82290582014301LGN01

**Table 4:** Supplementary Landsat images used for gap filling

<b>Year</b> <b>Path/Row</b>	<b>2004</b>	<b>2005</b>	<b>2015</b>
<b>228/57</b>	LT52280572004235CUB00	LT52280572005237CUB00	LC82280572015265LGN01
<b>228/58</b>		LT52280582005237CUB00	LC82280582015265LGN01
<b>229/57</b>		LT52290572005292CUB00	LC82290572015288LGN01
<b>229/58</b>		LT52290582005292CUB00	LC82290582015288LGN01

Other collected data used for creating the land cover maps for the prediction of the future LULC changes consisted of:

- a shape file of the Tapanahony River basin that was requested through the coordination of the SMNR program for this study by the GIS and Remote Sensing department

NARENA (Centre of Natural Resources and Assessment) of the Centre of Agricultural Research in Suriname (CELOS),

- a 2004 and 2014 roads layer map with a WGS84 reference system, downloaded from the OpenStreetMap website (2018), as an .osm file,
- shape files of the Suriname area, the Greenstone belt and settlements, with a WGS84 reference system, acquired from the SBB,
- shape files of the gold mining explorations within the study area that was received from the GMD,
- a proposed road layer for the Tapajai-Jaikreek hydropower project that was received from the staff of the state oil company ‘Staatsolie Ltd’,
- a Hansen Global Forest Cover 2016 tile (Hansen\_GFC-2016-v1.4\_last\_10N\_060W1) layer map for validation purposes that was downloaded from the earth engine and science website for High-Resolution global maps,
- a 30 m SRTM (Space Shuttle Radar Topography Mission) elevation data that features a much greater absolute vertical accuracy (Elkhrachy, 2017). This co-registered DEM provides a high quality resolution of 1 arc sec (30 mx30 m) and is publicly available and was downloaded from the USGS’s Earthexplorer site. The downloaded data was then projected to the UTM coordinate system zone 21 N, using ArcMap. (USGS, Products Archive, 2018c).

The following software was used for image processing and classification:

- ArcGIS 10.4

- Idrisi Selva version 17.02

Future LULC Modelling was performed using:

-Idrisi Selva: Land Change Modeler

### **3.3 Image enhancement of Landsat images**

Temporal satellite images from the study area were obtained from the NASA’s earth explorer website, from 2004 and 2014 (path 228/row57, path 228/row 58, path 229/row 57, and path 229/row 58). The image enhancement includes the processing of auxiliary data and image restoration on geometric, atmospheric and radiometric corrections to ensure spatial and temporal changes of the datasets, in order to improve the accuracy of LULC classification (Tiwari et al., 2014). The Landsat satellite data and shapefiles were geo-referenced to UTM Zone 21N North Projection reference system using the World Geodetic System 1984 (WGS-84 reference system). The bands from the Landsat sensors are located in the wavelengths of

the optical and infrared regions of the electromagnetic spectrum. To make a coherent superposition of the classified images, the final resolution utilized for the TM and OLI images was 30 meter to match the resolution as well for the SRTM DEM image (Figure 2).

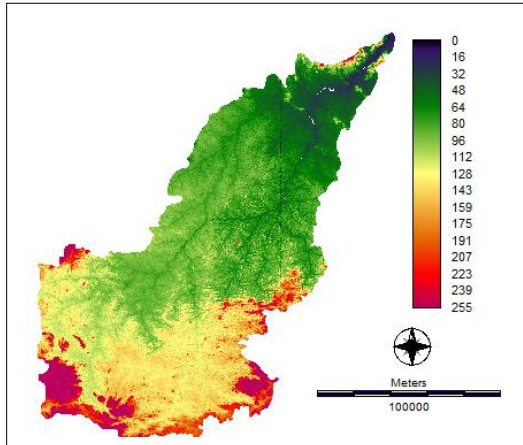


**Figure 2.** DEM of the study area (projected)

For the most part, the bands line up with some minor tweaking of the spectral ranges as it is shown in Table 5. In this study, all analysis were performed on the six non-thermal bands: three visible (0.45-0.52 $\mu\text{m}$ , 0.52-0.60  $\mu\text{m}$  and 0.63-0.69 $\mu\text{m}$ ) and three infrared bands (0.76-0.90  $\mu\text{m}$ , 1.55-1.75  $\mu\text{m}$  and 2.08-2.35 $\mu\text{m}$ ). Because of the thermal characteristics of band 6 of landsat 5 it was left out of further analysis (Tadesse, et al., 2014). Band 1 (Coastal/Aerosol), 8 (Panchromatic), 9 (Cirrus), 10 (TIR 1) and band 11 (TIR 2) of Landsat 8 were excluded of the analysis as the TM images do not contain them.

**Table 5.** Landsat 5 and Landsat 8 equivalent bands

Landsat 5			Landsat 8		
<u>Band Name</u>	<u>Bandwidth</u>	<u>Resolution</u>	<u>Band Name</u>	<u>Bandwidth</u>	<u>Resolution</u>
	<u>(<math>\mu\text{m}</math>)</u>	<u>(m)</u>		<u>(<math>\mu\text{m}</math>)</u>	<u>(m)</u>
Band 1 Blue	0.45 – 0.52	30	Band 2 Blue	0.45 – 0.52	30
Band 2 Green	0.52 – 0.60	30	Band 3 Green	0.53 – 0.60	30
Band 3 Red	0.63 – 0.69	30	Band 4 Red	0.63 – 0.68	30
Band 4 NIR	0.76 – 0.90	30	Band 5 NIR	0.85 – 0.89	30
Band 5 SWIR 1	1.55 – 1.75	30	Band 6 SWIR	1.56 – 1.66	30
			1		
Band 7 SWIR 2	2.08 – 2.35	30	Band 7 SWIR	2.10 – 2.30	30
			2		

### 3.3.1 Image restoration

Restoration techniques are preprocessing techniques for the removal of noise or flaws in imagery due to either sensor detection errors or natural noise from atmospheric effects (Eastman, 2012). The reflectance values recorded by Earth observing satellite sensors can be different from the surface reflectance values measured on the ground due to interference of gases and water vapor in the atmosphere causing absorption of energy at selected wavelengths. Therefore correcting for atmospheric contamination of the images is a significant procedure to convert or derive pixel values to the true surface reflectance value. A removal of atmospheric effects on remote-sensing imagery was an essential preprocessing step for the study area situated in a hilly and mountainous region and to increase the accuracy of the classification (Vanonckelen, et al., 2013, Prieto-Amparan et al., 2018). To maintain a comparable data set, radiometric correction was also applied on these images, since they were taken at different times, i.e. under different circumstances such as sun elevation and scene illumination (lillesand, et al., 2015). Geometric correction was already done for the Standard Terrain Correction (L1TP) Landsat images that incorporate a DEM for topographic accuracy and utilize ground control points for additional geometric accuracy. The radiometric and atmospheric correction of all Landsat images was performed using the Cos (t) model of the Atmosc module. This module is commonly used in several studies, to correct the atmospheric haze by converting the DN values to reflectance values (Myint, et al., 2010, Kinoti, K., 2017). The Cos (t) model takes into consideration the image band, sun elevation, the radiance conversion parameters, the optical thickness of the atmosphere, the scattering of the atmosphere (Eastman, 2012). Image mosaicking was performed after atmospheric correction of the images that allows them to join on the same satellite paths. The four images per year were mosaicked with the mosaic module, creating a larger composite image by spatially orienting the images and balancing the overlap regions by numerically averaging the individual pixels in the overlap regions (Warner, 2013). The study area was clipped out after the four images were merged together as demonstrated in Figure 3.



**Figure 3.** Image mosaicking

- (a) : Four band 4 images of the year 2004.
- (b) : The mosaicked band 4 image.
- (c) : The clipped out study area.

### 3.3.2 Cloud and cloud shadow masking

Masking clouds and cloud shadows from the 2004 and 2014 satellite images is useful because it reduces the usability and limits the interpretation of the data, by hiding parts of the territory. Removing clouds and cloud shadows also tends to remove spectral outliers from the images, causing spectral confusion resulting to pixel misclassification that turns in inaccurate image classification. Areas covered by clouds and cloud shadows must be quantified and localized in order to provide reliable information on spatial extent. Compared to other land cover types, the reflectance of cloud is much higher in almost all wavelengths, which makes clouds look “bright”. The spectral signatures of cloud shadows are very similar to other dark surfaces (e.g., rivers, wetlands, etc.). In some bands, clouds have the same spectral characteristics as some LULC classes, such as ‘Mines’ (Figure 4). Cloud and cloud shadow masking was performed manually on the eight main Landsat images because the machine- learning- based methods commonly fail to detect clouds and clouds shadow (Zhu et al.,2018). The elimination of clouds and cloud shadows was done, by manually delineating polygons around them to finally obtain one cloud and cloud shadow mask containing only the persistent clouds and cloud shadows, which are reported as ‘no data’ using the Reclass module. Finally the clouds and cloud shadows mask were removed from the images by filling the clouds and cloud shadows holes or gaps using the Overlay module in idrisi to stack images for each band that have been cloud-masked on the supplementary images for the relevant year. This was done until almost all the gaps in the main images were filled, producing cloud-free images for the years 2004 and 2014.

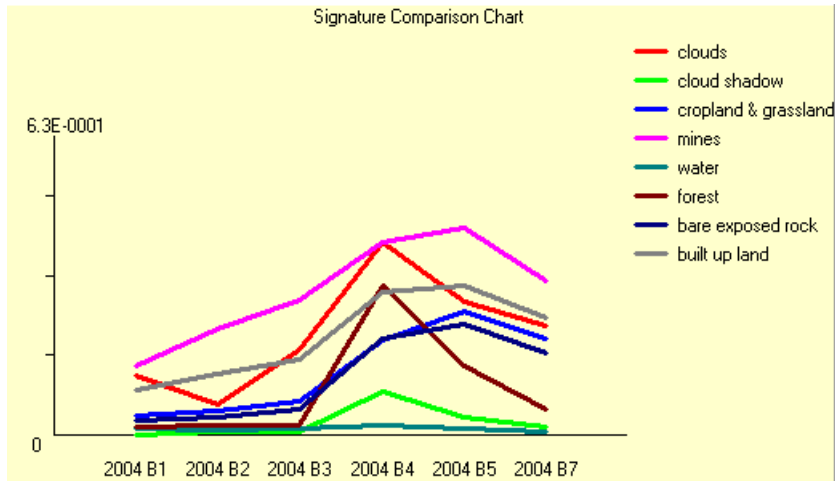


**Figure 4:** Signature comparison chart of clouds and cloud shadows with different LULC classes

### 3.4 Image classification

Several steps need to be followed for image classification in order to define the land-cover classes and to select training samples. The LULC classes of interest were derived from the USGS Anderson classification scheme (Anderson, et al., 1976) (Appendix 1), using level II classification with an image resolution of 30 meter. The land cover class ‘Forest’ is used in this study, since the ‘Secondary Forest’ class could not be distinguished easily from Primary Forest on the images. Reducing the numbers of classes can minimize the complexity of LULC transitions that achieve better performance during modeling (Li & Yeh, 2002). Based on the experience of existing state of the study area, 6 land-use classes were determined and used as reference for the classification process. The description of these classes are summarized and listed in Table 6.

**Table 6.** LULC classes with their description based on the Anderson classification scheme.

<b>Classes</b>	<b>Description</b>
1. Built-up land	Represent small scattered settlements with villages located on riverbanks and creeks, typically surrounded by plots of shifting cultivation at varying distances. It also includes paved and unpaved road networks.
2. Cropland and Grassland	Cropland represents land composed of a mosaic of small deforested lands, combined with fallow land at different stages of regeneration of the forest, intended for the practice of shifting cultivation (traditional agriculture). Grassland represents land covered with grass and other low vegetation (herbs, shrubs). Both Cropland and Grassland are used in combination because they are difficult to clearly distinguish from one another with regards to the Anderson level II classification.
3. Forest	Represents land covered primarily by trees, with a minimum tree crown cover of 30% , with the potential to reach a minimum canopy height at maturity in situ of 5 meters, and a minimum area of 1.0 ha. (SBB, 2017).
4. Water	Represents water bodies such as natural streams, rivers and creeks.
5. Mines	Represents current and abandoned strip mining, taken place along streambeds, in alluvial creek valleys on lower hill slopes and are typically elongated areas with multiple small digs (water ponds).
6. Bare exposed rock	Represents land that is irregular shaped by a solid aggregate of bedrock without vegetative cover.

Different false color composites were visually inspected with the composer module to identify the classes of interest. As the classes of interest were predetermined, a supervised classification method was used by identifying regions in the image, known as training sites. To analyze the spectral response pattern of each class, the training sites had to be digitized by drawing polygon format over the samples of the selected land-cover types. Although mining areas can include several land-use cover types, the criteria used in this study was to select only active

areas, i.e., open-pit mining areas that present high spectral levels in comparison to other classes. To avoid extensive misclassification with inactive mining areas that includes some vegetation mostly where small-scale mining occurs, the mining areas considered for this research included only active mining areas, i.e., barren soil (active exploitation areas) and associated water bodies. The Forest class includes light to dark dense vegetation areas and for the water class, natural rivers were sampled. Clear cut contains areas of Cropland and Grassland with regular geometry (shape) with little vegetation usually not far from rivers were also sampled for the training process. Attributing a specific integer identifier to each selected class was done using the digitizing tool. A vector file was created containing all the training polygons for the Makesig module in order to have the correct number of pixels per cluster for an accurate classification to occur. A general rule of thumb is that the number of pixels in each training set should not be less than 10 times the number of bands (Warner, 2013). Training sites were defined separately for each analyzed year consisting of the same information class. The Makesig module sets the minimum sample size per class as ten times the number of bands; in this case 60 pixels per signature. The bands used were bands 1-5, and 7 of landsat 5 and band 2-7 of landsat 8. The module generates pixels signatures and stores them in signature files where the digital number (DN) of each pixel is converted to radiance values making it possible to classify the various pixels on the map (Warner, 2013). The signature files contains statistical information about the reflectance values for each band for each site, derived from the digitized polygons. Once the Makesig module had finished, the SigComp module was run to visualize and compare the statistics of the training signatures (spectral response pattern). The SigComp graphs up the signatures over all the bands simultaneously as a spectral response pattern of mean reflectances as depicted in Figure 5.

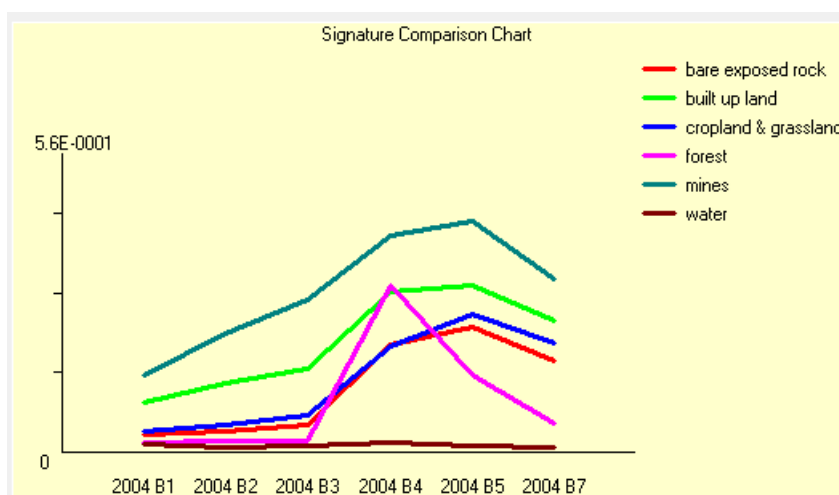


**Figure 5.** Comparison of the signatures of the LULC classes for the Tapanahony- River basin

The graph from Figure 5 suggest which signature group was the most dominant in the map. It can be notice that “Mines” has the highest reflectance values across the entire bands. Through comparison of the signatures of Figure 5, it can also be observed that the majority of the signatures are clearly distinguishable from each other and were not overlapping with other classes in most of all the bands, except for ‘Bare exposed rock’ and ‘Cropland and Grassland’ in band 3 and 4 in. Based on the comparison of the signatures, an appropriate hard automated classifier was selected, allowing proceeding with the classification process to produce a LULC map. The classifier examines each pixel’s reflectance and assigns it to the class which it resembles the most to perform the classification. The classifier could be chosen from the Fisher linear discriminant analysis (FLDA), and the Maximum likelihood (Maxlike), since they appear to be the most powerful classification techniques according to Eastman (2012). The Maxlike classifier work best when the training sites are strongly representative of each class and the sample size is large (Eastman, 2012). Maxlike was run first and the resulting map did not output well and showed signatures that were mixed and did not agree with the initial land cover training sites. The second classification module attempted was the Linear Discriminant Analysis (Fisher Classifier). The Fisher Classifier can perform exceptionally well when there are no substantial areas of unknown classes and when the training sites are strongly representative of their classes (Eastman, 2012). The Fisher module gave the best classification and was deployed in order to analytically generate land cover maps from the Landsat Tm imagery. In order to increase the accuracy of the final classified map and to facilitate the analyses, manual post-classification editing was performed to remove inconsistently identified features errors such as clouds and cloud shadows or to differentiate certain classes (Stuckenberg, et al., 2013). Pixels misclassified as ‘Bare exposed rock’, which fall near ‘Cropland and Grassland’ area, were reclassified as ‘Cropland and Grassland’. The manual editing was done based on advance knowledge knowing beforehand from reference data acquired from the Classification Map of the Republic of Suriname, shown in Appendix 2 (FAO Forestry Department, 2010 b) and produced digital deforestation maps of the SBB at the web portal of the GONINI National Land Monitoring System of Suriname.

### 3.5 Accuracy assessment

Congalton and Green (2009) have prepared the most common way to represent or determine the classification accuracy of remotely sensed data in the form of an error matrix. The error matrix compares the relationship between the reference data (ground truth) and the corresponding results of an automated classification (Lillesand, et al., 2015; Congalton, et al., 2009). Two important considerations for adequately assess the accuracy of remotely sensed data are reference data and sample size. Ground data or reference data must be collected. The ideal is that the reference is based on field data. Ground data collection is a difficult task, due to high cost of field sampling or to acquire high resolution images, making such data unavailable. A traditional solution to this problem is to use the cloud free landsat images as the reference image (Fung-Loy, 2014). As the study area is not rectangle shaped, a workaround method was developed using Arcmap 10.4. First by using the classified image as background layer were a large number of samples were generated using the random point's module. The next step for accuracy assessment was to overlay these stratified sample points on the original Landsat image and correct the point value of incorrectly classified sample points. The required number of sample points per class was 50 covering areas less than 4046, 86 km<sup>2</sup> except for the Forest class, to which a 100 sample points was given because of its largest area size measured with the Area module (Lillesand, et al., 2015; Congalton and Green, 2009). The following steps were taken to ensure that at least the 50 samples of each LULC class and the 100 sample size of the 'Forest' class did actually fall onto each LULC class:

1. from the study area, each LULC class area was isolated by creating Boolean layers of each class of interest in Idrisi,
2. each of the Boolean raster layers were digitized and merged into polygon features classes in ArcMap 10.4.,
3. the desired sample size of random points was created inside the polygon features classes,
4. the sample points were overlain and distributed randomly throughout an entire composite of a cloud - free landsat image (Figure 6). Different composites images could be utilized in the composite module and used to validate the sample points. Real color was represented using Landsat bands 321 and false color band 754, 432 and 543 were useful,
5. the land use and land cover was manually assigned by examining and recording the "true" land use or land cover class for each of the desired sample points. Because each random image generation is unique, the selection of the desired sample points will not be the same and

therefore the values of the associated class should be edited and corrected and hereafter stored in an attribute table of the point file.

6. the corrected points of all the LULC classes were merged into one single output dataset.

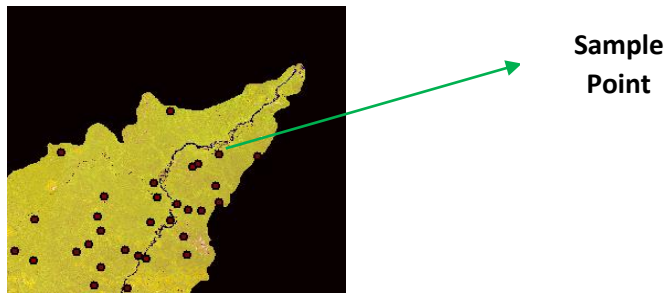


**Figure 6.** Random sampled points used for accuracy assessment

The corrected point shape file was imported in IDRISI using shapeIdr module. Using the DATABASE WORKSHOP, the ‘value’ column containing the class values was extracted as a vector file. The merged corrected points were used for the accuracy assessment. The Errmat module was used to generate the error matrix using the reference data and the classified images as inputs. The error matrix compares the relationship between the known (“true”) cover types from ground truth (columns) versus the mapped cover type from the classifier (rows). The following six statistics can be calculated from the error matrix: 1. overall accuracy, 2. Kappa Index of Agreement (KIA), 3. omission error, 4. commission error, 5. producer accuracy and 6. user accuracy. Correctly classified pixels (sample of locations) are listed along the major diagonal, while off-diagonal values represents errors of omission (in the column) and commission (in the row). The overall accuracy, which is defined as the proportion of all correctly classified objects and the total sample size, is computed by dividing the sum of the correctly classified pixels by the total number of reference pixels. In general an overall of larger than 85% is a commonly recommend target (Congalton and Green, 2009). User accuracy which is defined as the proportion of correctly classified objects within the total number of samples classified. The producer’s accuracy, which is defined as proportion of correctly classified objects to the reference samples of a class. Omission errors represent categories that were omitted when they exist on the ground, while the commission errors represent categories that were identified as existing on the ground when in fact they do not (Lillesand, et al., 2015). An alternative method of estimating classification accuracy is calculating the Kappa statistics (KIA) or Kappa coefficient ( $\kappa$ ), which is defined as the agreement of the classification results with the corresponding reference data occurring by

chance, and usually ranges between 0 and 1. A perfect agreement is evident when KIA equals 1; a value of KIA equals to 0 suggest that the agreement is no better than that which would be obtained by chance alone. Although there is no formal scale, the following levels of agreement are often considered appropriate for determining the extent of agreement as suggested by Cohen (Watson and Petrie, 2010):

poor if  $\kappa < 0.00$ , slight if  $0.00 \leq \kappa < 0.20$ , fair if  $0.21 \leq \kappa < 0.40$ , moderate if  $0.41 \leq \kappa < 0.60$ , good if  $0.61 \leq \kappa < 0.80$ , very good if  $\kappa \geq 0.80$ . In general the Kappa coefficient is multiplied by 100 to be expressed in percentages.

### **3.6 Past LULC change analysis between 2004 and 2014**

The process of developing a baseline model involves the analysis of a least two historical land use maps. The analysis allows the assessment of the historical changes between different land use classes. After the historical changes are analyzed, LCM allows for the modeling of LULC. The categorical LULC maps of year 2004 and year 2014 were used as input for the LCM. The 'Change Analysis' panel provides a set of tools for understanding the nature and extent of land cover change, including graphs of gains and losses, net changes and contributions experienced by any category. As this study focus was deforestation, mainly the transitions towards the 'Forest class' to Non-forest was analyzed. The change for the period 2004-2014 was used for the prediction phase. Maps of the areas where the changes have taken place were also produced for the period 2004-2014. Produced maps and graphs will gave an idea of how the area has changed in the past.

#### **3.6.1. Driver variables**

Changes in forest cover occur due to land use change, caused by different drivers or phenomena. For the transition under investigation, from Forest to Non-Forest, a series of potential drivers of change are identified and tested for its relevance in the process of change. The main driving force behind deforestation in Suriname is the Artisanal Small scale Gold Mining (ASGM), which is the main source of income for the communities in the Greenstone belt and is usually practiced in the close vicinity of rivers (Unique, 2016). Figure 7 shows the gold exploration layers situated at the north part of the Tapanahony River basin, were most of the ASGM is taken place near the Sela and the Toso creek. Mining usually practiced near rivers and designated exploration areas of the Greenstone belt, indirectly leads to some development such as the expansion of paved and unpaved roads. It is reasonable to consider

the proximity of roads as a direct cause for deforestation, while nearby creeks, gold exploration areas and the Greenstone belt as underlying causes. The settlements on Built-up lands within the Tapanahony river basin are mostly located along the rivers were shifting cultivation (activities regarding changes from 'Forest' to 'Cropland and Grassland') and alluvial gold mining are mostly practiced. Driving forces behind deforestation cannot be translated spatially, therefore the driver variables were modeled and created as distance maps using the Distance module in Idrisi. There are two types of driver variables: static or dynamic. Static drivers are expressing aspects of basic suitability for the transition under consideration and do not change during iterations for the predictions of future trends. Dynamic variables are time-dependent drivers that do change over time. Dynamic variables are recalculated at each iteration during the course of prediction. The driver variables test to confirm whether or not they hold explanatory power for the transition, is based on a contingency analysis. They need to be transformed with the evidence likelihood transformation or separated by Boolean layers (Eastman, 2012). In this study Boolean layers were used to create distance maps and transformation was not required. Boolean variables were created from the categorical 2004 map for the 'Built-up land', 'Cropland and Grassland', 'Mines', and were thereafter modeled as distance maps. Distance maps were also created for the Greenstone belt, gold exploration, roads layer of 2004, river and settlements. These different driver variables are presented in Table 7 and Figure 8. The unit of the distance variables is in meters. For a given set of input images, the minimum distance to a feature is calculated for every cell (Figure 8) The Distance module calculates the true Euclidean distance of each cell and the nearest of a set of target cells as specified in a separate image (Eastman, 2012). The driver variables were tested in order to better understand the forces of change and model the transition of the LULC changes between 2004 and 2014.

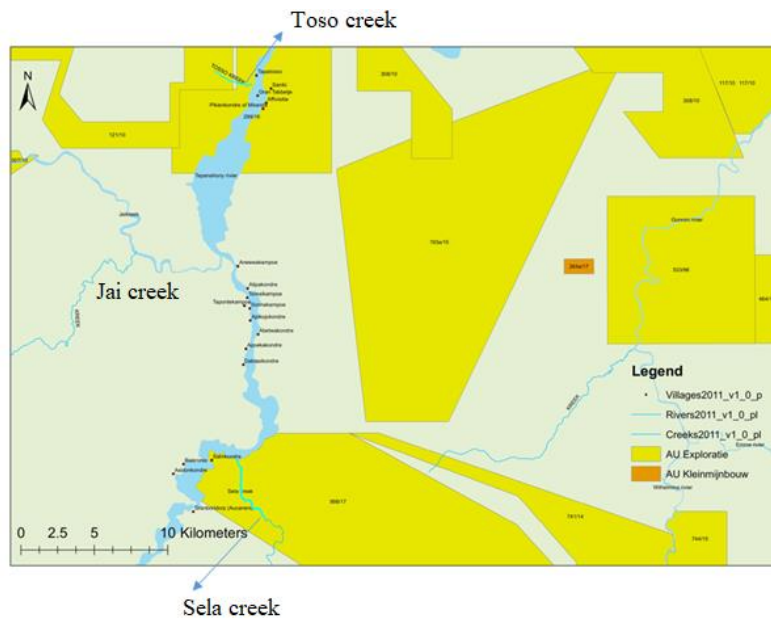
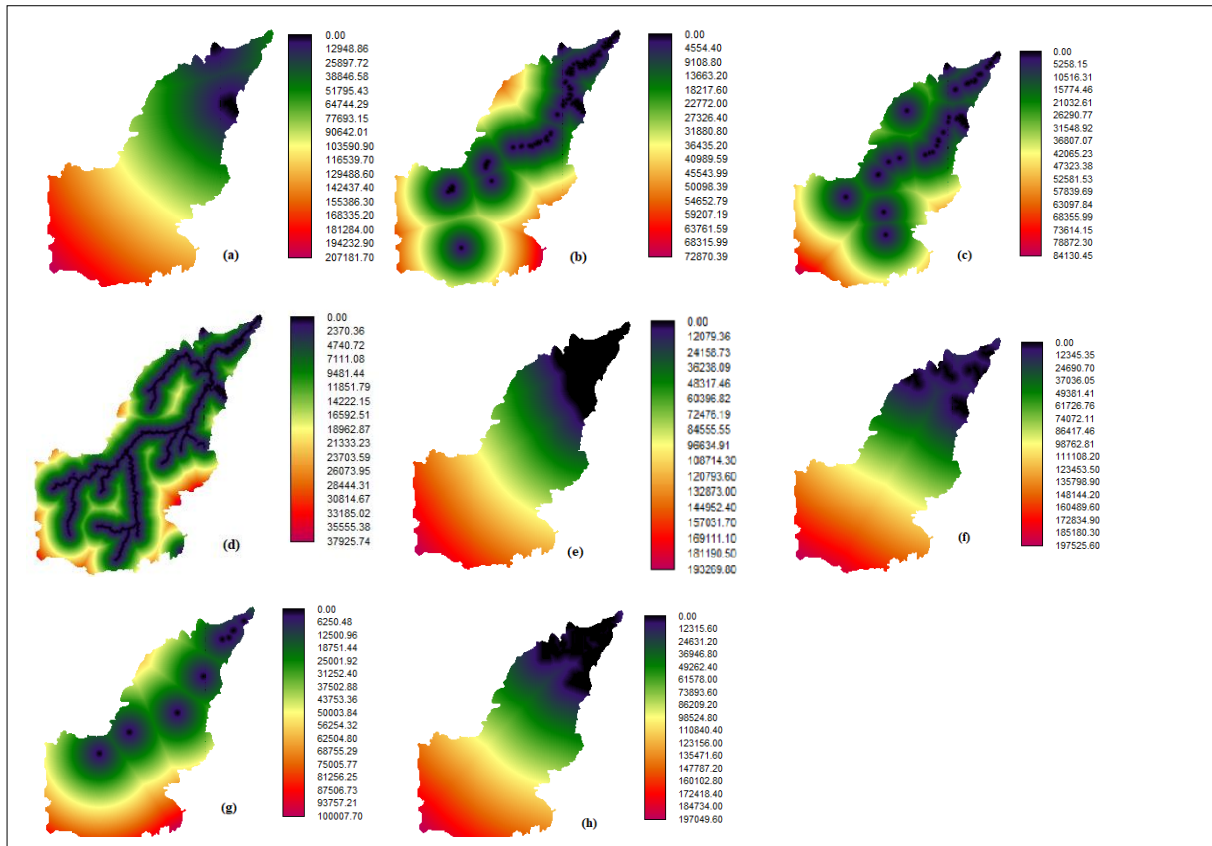


Figure 7: Gold exploration layers along the Toso and the Sela creek (GMD, 2018).

**Table 7.** Possible driver variables

Possible driver variables	Type of variable
1. Distance to Cropland and Grassland in 2004	Dynamic
2. Distance to Mines in 2004	Dynamic
3. Distance to Built-up land in 2004	Dynamic
4. Distance to Greenstone belt	Static
5. Distance to rivers	Static
6. Distance to settlements	Static
7. Distance to Gold exploration	Static
8. Distance to roads in 2004	Dynamic



**Figure 8.** Possible driver variables modeled as distance maps

(a) distance to mines, (b) distance to cropland & grassland, (c) distance to built-up land,

(d) distance to rivers, (e) distance to greenstone belt, (f) distance to roads

(g) distance to settlements, (h) distance to gold exploration

### 3.6.2 LULC transition modeling

Using past land transition information and incorporating explanatory variable maps that might drive or explain such change, LCM can create layer expression of transition potential in other words the likelihood of a pixel changing from one type of land cover to another type in the future. To model the potential of land transitions, the *Transition Potentials* tab was used to create 3 sub-models of interest namely from ‘Forest to Mines’, ‘Forest to Cropland and Grassland’ and ‘Forest to Built-up land’. A requisite to explain and model the historical changes or transitions between 2004 and 2014 with LCM, is to test the significance or explanatory power of the potential driver variables previously identified, enabling them to

make the transitions of changes possible. The measure of association used in the test is the Cramer's V. According to Eastman a high Cramer's V designates that the potential explanatory or driver variable power is good, when Cramer's V > 0.40 and it is useful when Cramer's V > 0.15, but it does not assure the certainty of a strong performance regarding the complexity of their association or correlations (Eastman, 2012). A low Cramer's V is also a good indication that the concerning driver variable is not useful and can be thus discarded (Eastman, 2012). The 'distance to road' dynamic driver was tested and the information was used on purpose despite its Cramer's V value, to create the 3 sub-models of interest, because of its requirement for the dynamic road modeling in the prediction phase. Various drivers were tested with different combinations for each of the sub-model and added to the transition sub-model. Each transition can be modeled with either logistic regression, sim weight or a multi-layer perceptron (MLP) neural network available in LCM, resulting in a potential map for each transition, an expression of time specific potential for change. MLP neural network has the advantage that it can run multiple transitions per sub model whereas the sim weight and logistic regression can only run one transition per sub model. The model calibration was performed using the MLP with the default parameter as it perform the best in modeling transitions and it generally gives more accurate results requiring the least user intervention with a shorter runtime (Atkinson, 1997, Eastman, 2012, Mozumder et al., 2016). Additionally some insight is given about the performance of the drivers, the overall accuracy rate and the average skill of the sub-model. Generally an accuracy rate of approximately 80% and a skill between -1 and 1 should be achieved, with 1 being the perfect prediction, a negative skill indicating that the model is doing worse than chance (Eastman, 2012) and a skill of 0 means the modeling is no better than chance. Besides the average skill and accuracy, the individual model skill breakdown of the modeled historical change is also an important factor to be observed. The model should be run again, if the transition skill is to low or the accuracy rate is less than 75% (Eastman, 2012). The combination of the driver variables produces a map or a transition potential map, which indicated the areas with the lowest and highest potential for deforestation occurrence varying between 0 and 1, with 0 as the lowest and 1 being the highest potential to transition. The produced historical transition potential maps can be used to predict future LULC changes.

### **3.7 Model comparison and validation**

The drivers were tested for the study area in order to better understand the forces of change and to produce the historical transition potential maps. The LCM uses this information to model the prediction for the years 2020, 2030 and 2040. The models need to be validated before predicting the LULC future trends by evaluating the performances of the LCM. The evaluation is done by producing a predicted LULC map for the year 2016 with LCM and to compare or validate its quality with an LULC map of reality. The year 2016 was chosen as the validation year, because of the availability of a high resolution reference map of the cloud free image: 'Hansen\_GFC2016\_last\_10N\_060W' for the year 2016. The cloud free composite image was downloaded from the 'High – Resolution Global maps of 21<sup>st</sup> - Century Forest Cover Change' website. The Hansen map of 2016, was classified and assumed as the map of reality. The validation is done by comparing the relationship between the reference map of Hansen and the predicted map of 2016, by assessing the accuracy with the Errmat module. The data of the Hansen map of reality is proposed as the reference data. The result of this validation was the output of the Errmat matrix in terms of the overall accuracy and the KIA to assess how accurately the predicted map was produced by the LCM. Another method to assist in the validation process was through the Validation module of Idrisi. This module compares the agreement of the predicted LULC maps of 2016 and the LULC map of reality for 2016. The Validation module uses several forms of Kappa statistics to express the validation: Kappa for location, Kappa for no ability (K-no) and the Kappa standard. According to Pontius (2000), the standard Kappa offers no useful information because it mixes up quantification error with location error, while the K-no can specify the quantity accurately. Unlike the K-no and the Kappa standard, the Kappa for location its ability to specify spatial allocation is better. If the location of the prediction is of interest, then the Kappa for location can be a more useful criteria for validation, than either K-no and Kappa standard (Pontius, 2000). There is allocation agreement if there is no amount of difference between the reference map and the comparison map, which is due to optimal match of spatial allocation of the categories, given the proportions of the categories in both maps (Pontius, 2000).

## 3.8 Change prediction maps

### 3.8.1 Change prediction Process

The dynamic change prediction relies on the historical transitions and models forward to a specified future date. The quantity of change can either be modeled through a Markov Chain analysis or by providing a transition probability matrix. This procedure determines exactly how much land would be expected to transition from the later date to the prediction date based on a projection of the transition potentials on the past trends into the future where after the LCM creates a transition probability file or matrix. This matrix can be edited, however as future quantities are not know beforehand these adjustment are not meaningful and are not taken forwards in future predictions, because it will effect the quantity. In the *Change Demand Modeling* panel of the *Change Prediction* tab, the predicted year needs to be specified. The amount of change for

2020, 2030 and 2040 was predicted, based on the amount of LULC change between 2004 and 2014. The three transition of interest were added in the *Dynamic Road Development* and *Change Allocation* panel of the LCM, in order for the stochastic highest transition potential end point generation mode to enable the connection with areas having a high transition potential (Eastman, 2012). The prediction of the future LULC was done in recalculation stages that indicates the frequency with which the dynamic elements are recalculated. LCM allows for the specification of the number of reassessment stages during which dynamic variables are updated. At each stage, the system also checks for the presence of planning interventions such as proposed roads, that may alter the course of development in the change prediction process as described in chapter 3.8.2. Two recalculation stages of 1 year and 3 years were respectively given for the prediction from 2014-2016 and 2014-2020. For the prediction from 2014 -2030, 4 recalculation stages of 4 years were given and for the prediction from 2014-2040, 2 recalculation stages of 13 years were allocated. In the *Change allocation* panel, the options '*dynamic road development*' and '*apply infrastructure*' were chosen and enabled respectively for scenario 1 and scenario 2. Scenario 1 was the business as usual scenario and was modeled for the years 2016, 2020, 2030 and 2040. In scenario 2 the impact of the proposed Tapajai roads on the transitions of interest was only modeled for the years 2020, 2030 and 2040, as the year 2016 was only used to validate the model and therefore the prediction was not needed. The basis roads layer was the road layer from 2004 and was incorporated in the LCM process. The road layer contains the end part of the Staatsolie secondary road of  $\pm 24$  km and unpaved tertiary roads with a total length of  $\pm 100$  km. Figure 9 shows the proposed primary road of

the Tapajai Project, the Staatsolie secondary road and the tertiary roads used for the prediction process. New roads will develop out from this basic layer under scenario 1, except primary roads since they do not exist within the study area. Primary roads can grow by extending their endpoints, secondary roads can grow as new branches of primary roads and they can extend themselves, while tertiary roads grows in similar manner (Jiang, 2007). Two important spatial properties of a road network necessary for the prediction are the road growth parameters: road spacing and road length. Road length indicates the maximum length a road class will grow in each dynamic stage. The actual length of any new segment will fall randomly within that range. Road spacing indicates the frequency, specifically minimum distance, with which roads are generated along a route of superior class (Jiang, 2007). Both the averages of road space and length were measured and rounded up. For the Secondary and tertiary road an average road length of respectively 20 km and 4 km was maintained and for road spacing an average of respectively 45 km and 18 km was maintained. The stochastic highest transition mode assumes that the growth of an individual road can be defined as two consecutive processes as follows: the model first identifies endpoints of new roads; it then generates routes that link endpoints to existing road (Jiang, 2007). The skip factor parameter was set to 1 meaning that roads will be built at every recalculation stage. The prediction output as a result of conducting scenario mapping, is a soft prediction map which is a continuous map of vulnerability to change for the selected set of transitions and it provides a comprehensive assessment of change potential. Another result of the prediction process is a hard prediction map that is a single realization of a definite LULC map (Eastman, 2012).

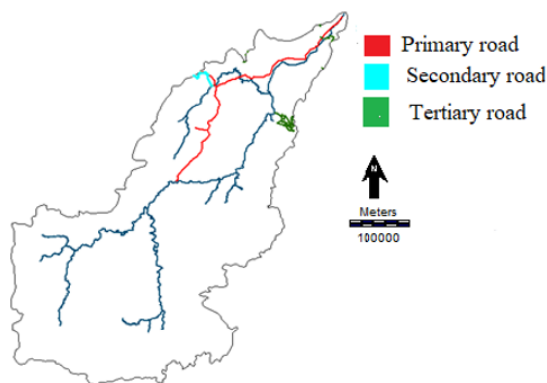


**Figure 9.** The primary (proposed), secondary and tertiary roads within the study area

### 3.8.2 Proposed roads interventions

The impact of roads on land use in adjacent and distant territories depend on a number of variables that are frequently included in land use modeling for example distance to types of transport infrastructure and to population settlements. The closer the area is located to infrastructure the more deforested it will be in course of time when predicting changes (van Dijck, 2014). Planning interventions include infrastructural changes such as proposed roads that may alter the course of development when modeling future scenarios, are specified in the *Planned Infrastructure Changes* panel of the *Planning* tab. This panel is used together with the *Change Allocation* panel of the *Change Prediction* tab, because it checks infrastructure changes with each stage of the prediction (Eastman, 2012). In this study, the road layer of 2014 was added to the model as planning intervention for both scenarios, while the proposed primary road layer of the Tapajai project was added to the model for scenario 2. The Tapajai project includes the diversion of the water-flow of the Tapanahony river and the Jai Kreek that would contribute to hydro-energy production of the Brokopondo storage lake in the north of the country (Boksteen, 2009). This project was on hold for several times but since it is mentioned in the Policy Development Plan 2017-2021 of Suriname (Policy Development Plan, 2017), there might still be a possibility for it to be implemented, because of projected energy demands. The project will provide increase electrical generation and improved supply reliability for the entire country and therefore is of national importance (Environmental Research Management, 2011). The *Dynamic road* modeling updates new road features in the prediction process under scenario 1 for the years 2016, 2020, 2030 and 2040. The *Apply Infrastructure Changes* needs to be enabled before running the model for the planned infrastructure at specified dates in the prediction process under scenario 2 for the years 2020, 2030 and 2040.

The different steps starting from the pre-processing of landsat images, classification, change analysis, transition potential modelling, calibration and change prediction are presented in a flowchart in Figure 10.

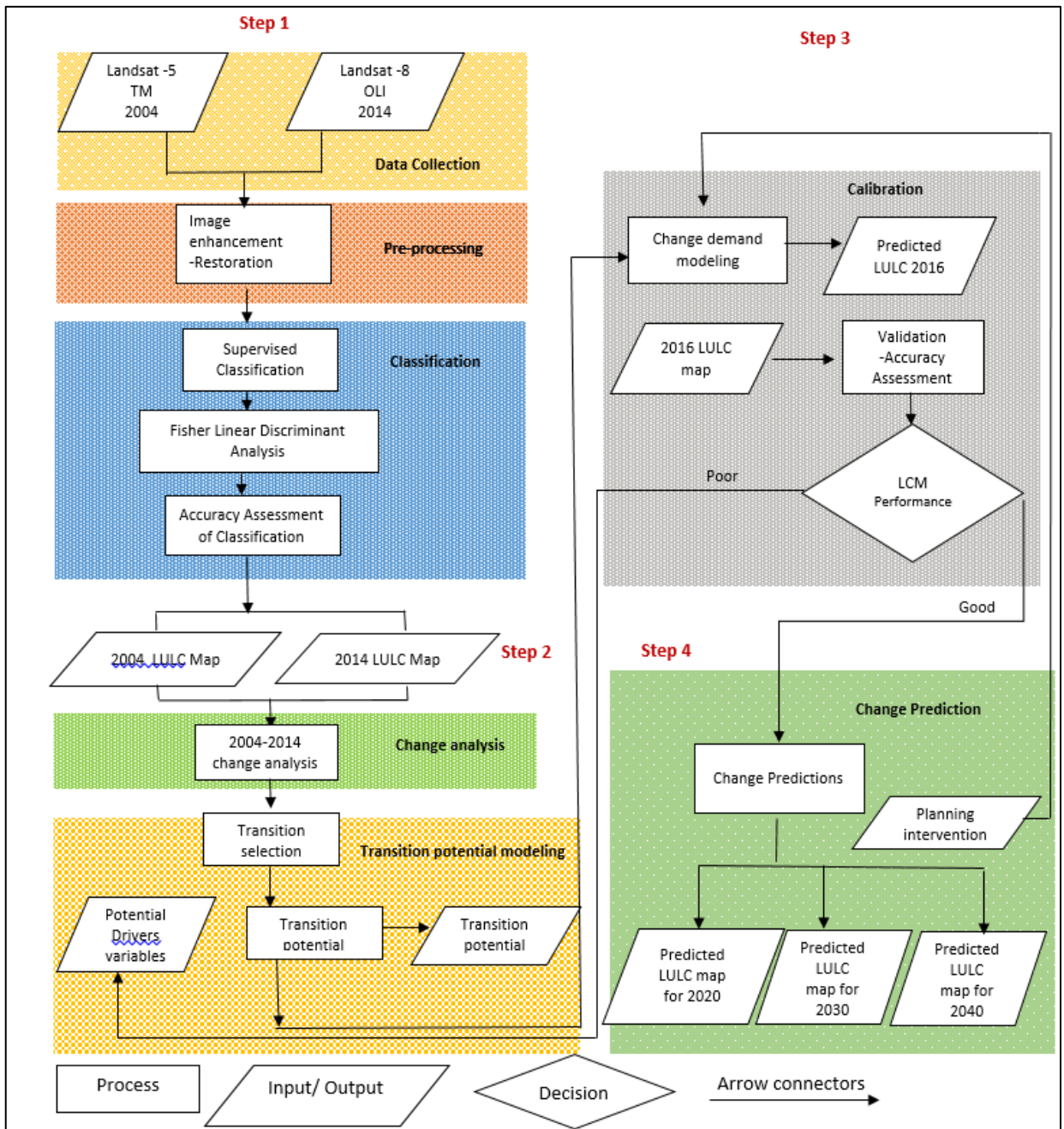


**Figure 10:** Steps in the flowchart to address the LULC analysis and prediction process

## 4 Results

### 4.1 Image classification

The results of the FLDA classification, with the manual post-classification correction resulted in the categorical maps depicted in Figure 11. Little or less LULC changes can be visually determined when comparing the subsequent maps of 2004 and 2014.

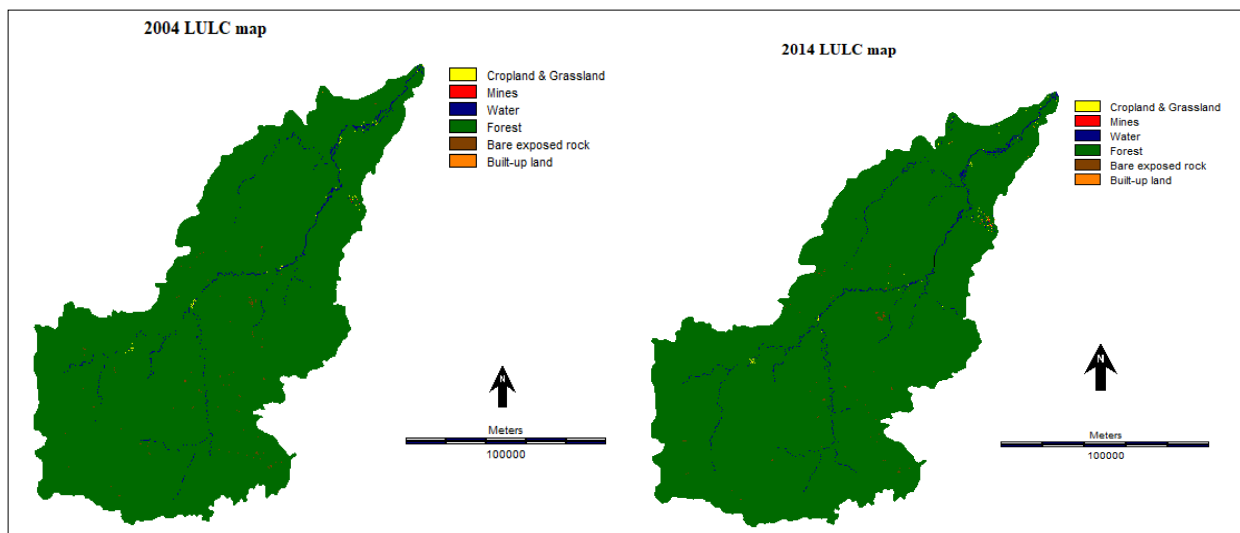


**Figure 11.** The classified LULC map of the year 2004 and 2014

#### 4.2 Accuracy assessment

To compare the classified map with the reference data, an error matrix was produced. The error matrix for the year 2014 is shown in Table 8.

**Table 8.** Error matrix for the landsat 2014 classification map

		Reference points 2014						Total	Error Commission
		Cropland & Grassland	Mines	Water	Forest	Bare exposed rock	Built-up land		
2014	Cropland & Grassland	47	0	1	1	0	1	50	0.0600
	Mines	1	36	0	0	0	6	43	0.1628
	Water	0	0	39	8	0	1	48	0.1875
	Forest	1	0	1	105	2	0	109	0.0367
	Bare exposed rock	0	0	0	0	48	0	48	0.0000
	Built-up land	0	1	0	0	0	49	50	0.0200
Total		49	37	41	114	50	57	348	
Error of Omission		0.0408	0.0270	0.0488	0.0789	0.0400	0.1404		

It can be seen in the error or confusion matrix that bare exposed rock had the best classification accuracy from all the classes, while water and mines had the most number of pixels misclassified in terms of errors of commission. Areas that were committed into mining class

were manually removed during post classification procedure, from vector layers, whereas water bodies and bare soil that are directly derived from mining operation were re-classified into mining class. This procedure is dependent on the user's interpretation to distinguish mining areas from those of other uses, which can lead to omission and commission errors in particular small-scale mining (Souza-Filho, 2018). The overall accuracy and the Index of Agreement (KIA) are listed in Table 9. The error matrix of year 2004 is given in Appendix 3. The year 2014 was classified the best related to year 2004. Both years had a very good or strong agreement as the KIA was greater than 80%.

**Table 9.** Overview of the accuracies and KIA's

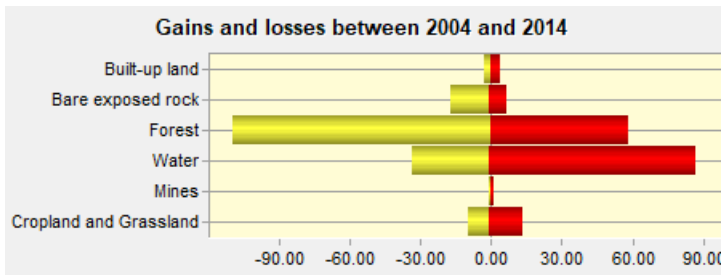
<b>Year</b>	<b>Overall Accuracy (%)</b>	<b>Overall KIA (%)</b>
<b>2004</b>	<b>90.28</b>	<b>87.15</b>
<b>2014</b>	<b>93.10</b>	<b>91.43</b>

#### **4.3 Past LULC change analysis between 2004 – 2014**

Based on the outcomes of Table 10 and Figure 12, on gains and losses it can be seen that water followed by Forest, Bare exposed rock and Cropland and Grassland shows the largest net changes in km<sup>2</sup>. Water showed an increasing trend and was the major overall gainer in the period 2004-2014, followed by Cropland and Grassland with an area gain of 4.00 km<sup>2</sup>, which is 3.42% per year. Forest showed a loss of 50.86 km<sup>2</sup>, which is 0.03% per year. Figure 12 shows declines in Forest towards the classes of interest: Cropland and Grassland, Mines and Built-up land.

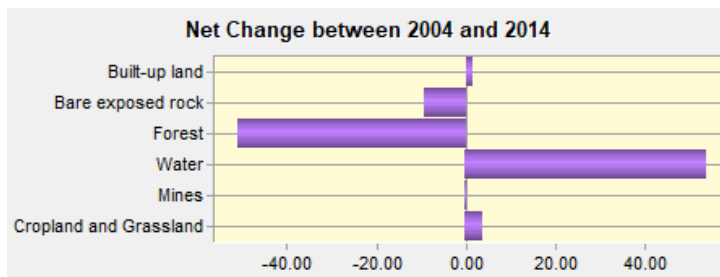
**Table 10.** Changes occurring between 2004 and 2014 in the Tapanahony River basin

<b>Classes</b>	<b>2004 area (km<sup>2</sup>)</b>	<b>Losses (km<sup>2</sup>)</b>	<b>Gains (km<sup>2</sup>)</b>	<b>Net change (km<sup>2</sup>)</b>	<b>Net change/year (km<sup>2</sup>)</b>	<b>Net change/year (%)</b>
Forest	19869.24	-109.02	58.17	-50.86	-5.09	-0.03
Cropland and Grassland	11.68	-9.82	13.82	4.00	0.40	3.42
Mines	1.25	-1.06	1.48	0.42	0.04	3.36
Built-up land	3.41	-2.61	4.18	1.57	0.16	4.69
Water	185.92	-33.38	87.72	54.35	0.16	0.09
Bare exposed rock	31.40	-16.96	7.47	-9.49	-0.95	-3.03



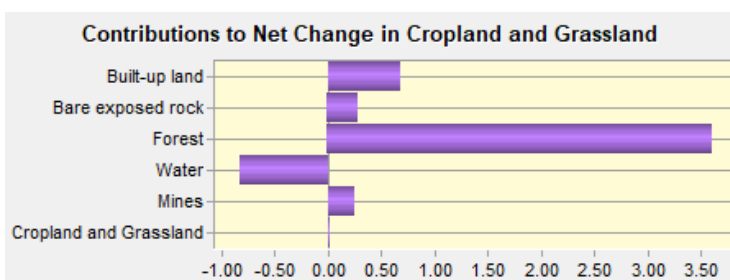
**Figure 12.** Gains and losses occurring between 2004 and 2014 in the Tapanahony River basin.

Figure 13 presents the net change graph by category Forest and presents the changes occurring in the study area between 2004 and 2014. Declines in Forest towards Cropland and Grassland, Mines and Built-up land can be observed. From 2004 to 2014, deforestation was the main change in the Tapanahony River basin, as Forest showing a loss of 50.86 km<sup>2</sup>, while Cropland and Grassland, Water, Built-up land and Mines shows and increasing trend.



**Figure 13.** Net change in km<sup>2</sup> in the Tapanahony River basin between 2004- 2014

Forest shows a positive contribution to Cropland and Grassland during 2004-2014, in other words Forest is declining at the expense of Cropland and Grassland for 3.63 km<sup>2</sup>, as showed in Figure 14.



**Figure 14.** Contributors to net change in cropland & grassland (km<sup>2</sup>)

Forest shows a positive contribution to Built-up land during 2004-2014, meaning a loss of 2.58 km<sup>2</sup>, while Cropland and Grassland showed a negative contribution to built-up land contribution according to the contributions to net change graph results as presented in Figure 15.

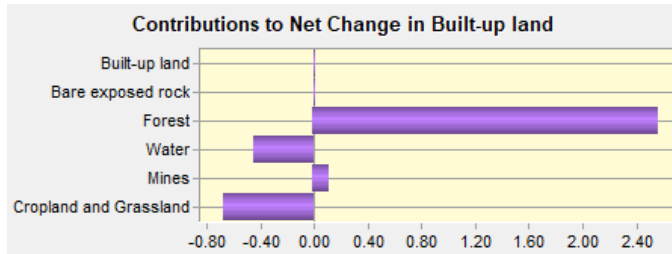


**Figure 15.** Contributors to net change in Built-up land (km<sup>2</sup>)

Forest has mainly transitioned to Mines and declined at the expense of mines for 0.88 km<sup>2</sup> as graphed in Figure 16, while Cropland and Grassland showed a negative contribution to mines.

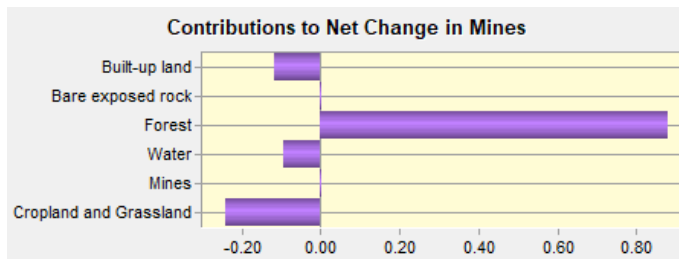


**Figure 16.** Contributors to net change in Mines (km<sup>2</sup>)

All of the above contribution to net changes graphs led to consider the following transitions of interest with regards to deforestation:

- Forest to Mines
- Forest to Cropland and Grassland
- Forest to Built-up land

From Table 11, it can be seen that the main changes of interest between 2004 and 2014 was the total forest area lost to ‘Cropland and Grassland’, ‘Mines’ and ‘Built-up land’ of 7.09 km<sup>2</sup>, with a forest loss of 3.63 km<sup>2</sup> to Cropland and Grassland, followed by 0.88 km<sup>2</sup> of forest that was lost to ‘Mines’ and 2.58 km<sup>2</sup> lost to ‘Build-up land’. The Area module of idrisi gave a clear indication on how the surface areas of each LULC category changed over the time period 2004-2014, which is illustrated in a bar graph in Figure 17.

**Table 11.** Amount of area changed per transition

Transitions	Area of changes (km <sup>2</sup> )
Forest to Built-up land	2.58
Forest to Mines	0.88
Forest to Cropland & Grassland	3.63

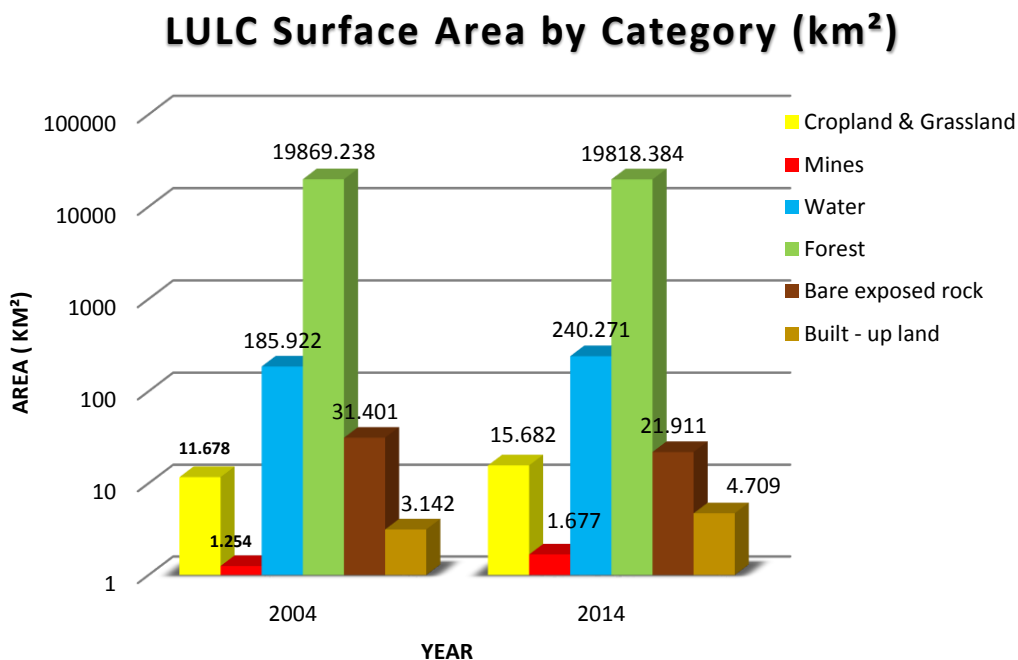


**Figure 17.** LULC Surface Area by Category

## 4.4 Transition potential modeling

### 4.4.1 Driver testing

The Cramer V was obtained from the *Test and Selection of Site and Driver Variables* tab in LCM and is tabulated in Table 12. Based on the Cramer's V criteria to be > 0.15 it can be examined that distance to Cropland and Grassland, distance to Built-up land, distance to rivers and distance to settlements had a Cramer V larger than 0.15 and are useful for the Forest class.

**Table 12.** Driver variables tested with the Cramer’s V

Driver variables	Cramer's V by Classes					
	Cropland and Grassland	Mines	Forest	Built-up land	Water	Bare exposed rock
Distance to cropland and grassland in 2004	0.1229	0.0525	0.2451	0.0690	0.2208	0.0338
Distance to Mines in 2004	0.1177	0.0963	0.1087	0.1142	0.0891	0.0480
Distance to Built-up land in 2004	0.1432	0.0713	0.2325	0.0917	0.2015	0.0260
Distance to rivers	0.0667	0.0325	0.4123	0.0411	0.4256	0.0203
Distance to settlements	0.0688	0.0251	0.1677	0.0248	0.1632	0.0304
Distance to roads	0.0782	0.0530	0.1132	0.0707	0.0973	0.0526
Distance to Greenstone belt	0.0513	0.0239	0.1019	0.0379	0.0949	0.0541
Distance to Gold exploration	0.0514	0.0262	0.0998	0.0392	0.0922	0.0623

#### 4.4.2 Transition sub-model Forest to Cropland and Grassland

The sub-model from ‘Forest to Cropland and Grassland’ was tested and run with different combination of driver variables as presented in Table 13. The sub-model achieved an overall accuracy rate of 90.91 % and an average skill of 0.8181. The accuracy was > 80% meaning that the sub-model Cropland and Grassland was an adequate model and good in modeling the transition from ‘Forest to Cropland and Grassland’. The model skill breakdown by transition showed that that the model was 82.01% better than chance at predicting the transition ‘Forest to Cropland and Grassland’. The most influential variable for this process was the variable distance to river and the least influential was the variable distance to settlements. The combination of these drivers produces a map through the MLP run, named as the Transition Potential Map from ‘Forest to Cropland and Grassland’ as presented in Figure 18. The map indicates areas of Forest with High (values close to 1) or Low (values close to 0) potential to deforestation occurrence. Areas in red and orange have high transition potential and areas in dark blue and green low transition potential. The regions in dark grey to black do not have any transition potential.

**Table 13.** Accuracy, skill and driver assessment of the Sub-model ‘Forest to Cropland and Grassland’

Transition Sub-Model	Overall Accuracy (%)	Average Skill Measure	Skill of Transition	driver variable with influence order from 1-5*				
				Distance to Cropland and Grassland	Distance to roads	Distance to settlements	Distance to rivers	Distance to Built-up land
Forest to Cropland and Grassland	90.91	0.8181	0.8201	4	3	5	1	2

\* 5: least influential

\* 1: most influential

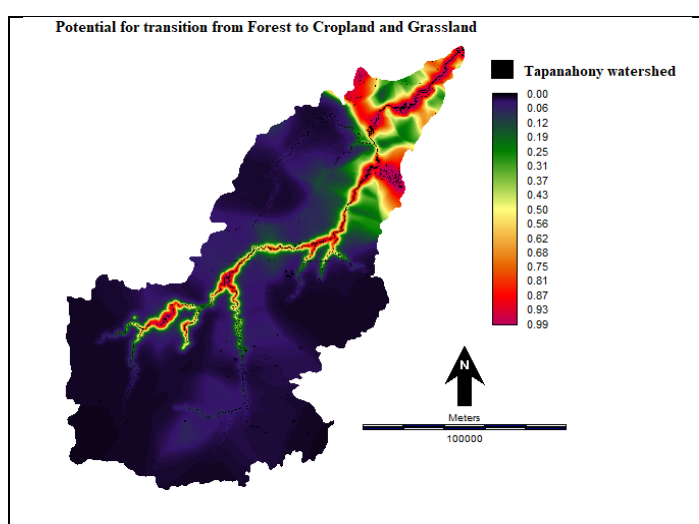


**Figure 18.** Transition Potential Map: Forest to Cropland and Grassland

#### 4.4.3 Transition sub-model Forest to Mines

The sub-model ‘Forest to Mines’ was run and tested with different combinations of driver variables as presented in Table 14. The sub-model achieved an overall accuracy rate of 98.21% and an average skill of 0.9642. The accuracy rate of this model was > 80%, meaning that the sub-model ‘Mining’ was good in modeling the transitions from ‘Forest to Mines’. The model skill breakdown by transition showed that the model was 96.67% better than chance at predicting the transition ‘Forest to Mines’. Distance to Mines was the most influential variable, followed by Distance to road and Distance to gold exploration and the least influential was the variable Distance to Built-up land. The areas with the potential to transition from ‘Forest to

Mines’ are presented in Figure 19. The higher probabilities for the transition from ‘Forest to Mines’ have similar contours to the Mines layers of 2004. The North region of the study area presents the highest transition potential to deforestation occurrence in the close vicinity of the mining areas.

**Table 14.** Accuracy, skill and driver assessment of the Sub-model ‘Forest to Mines’

Transition Sub-Model	Overall Accuracy (%)	Average Skill Measure	Skill of Transition	driver variable with influence order from 1-8*				
				Distance to mines	Distance to Greenstone belt	Distance to gold exploration	Distance to road	Distance to river
Forest to Mines	98.21	0.9642	0.9667	1	4	3	2	7
				Distance to settlements	Distance cropland and grassland	Distance to built-up land		
				5	6	8		

\* 1: most influential  
 \* 8: least influential

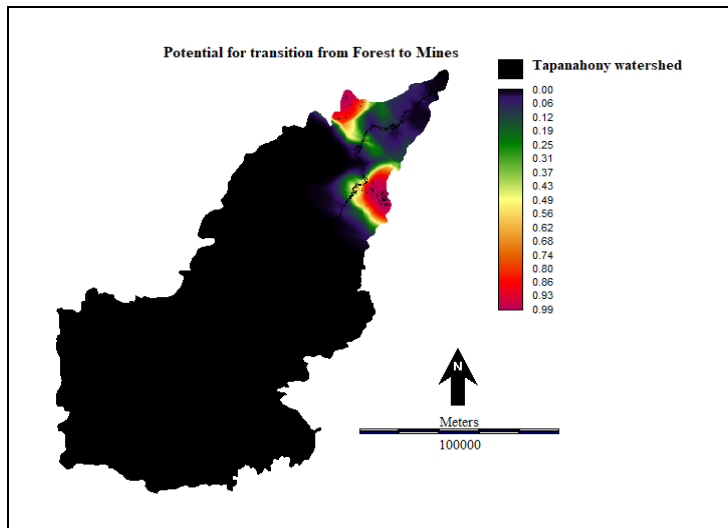


**Figure 19.** Transition Potential Map: Forest to Mines

#### 4.4.4 Transition sub-model Forest to Built-up land

The sub-model ‘Forest to Built-up land’ was tested and run with different combination of driver variables as presented in table 15. The sub-model achieved an overall accuracy rate of 93.84% and an average skill of 0.8769. The accuracy was > 80% meaning that the sub-model

‘Forest to Built-up land’ was an adequate model. The model skill breakdown by transition showed that that the model was 90.21% better than change at predicting the transition ‘Forest to Built-up land’. From the model run the Distance to Greenstone belt was the most influential variable and the least influential variable for this process was the variable Distance to road. The areas with the potential to transition from ‘Forest to Built-up land’ are shown in Figure 20. The North part of the study area presents the highest transition potential to deforestation occurrence. Areas in red, orange and dark pink have high transition potential in the close vicinity of the greenstone belt. The regions in black do not have any transition potential to deforestation occurrence.

**Table 15.** Accuracy, skill and driver assessment of the Sub-model ‘Forest to Built-up land’

Transition Sub-Model	Overall Accuracy (%)	Average Skill Measure	Skill of Transition	driver variable with influence order from 1-7*				
				Distance to Built-up land	Distance to Greenstone belt	Distance to gold-exploration	Distance to road	Distance to river
Forest to Built-up land	93.84	0.8769	0.9021	3	1	2	7	4
				Distance to settlements	Distance to mines			
				5	6			

\* 1: most influential  
\* 7: least influential

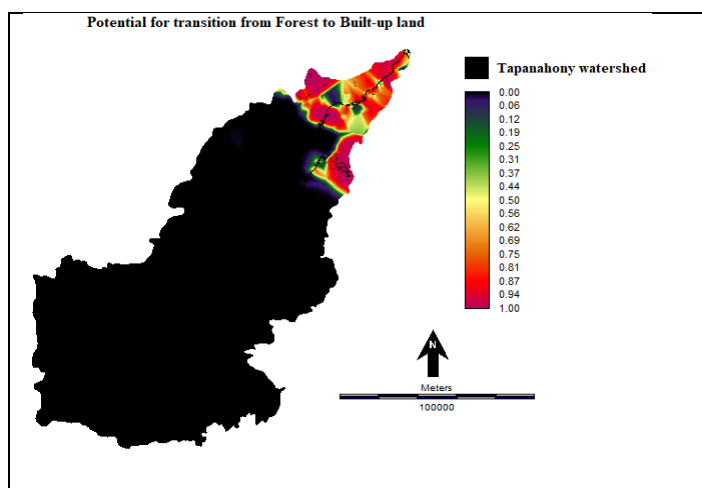


**Figure 20.** Transition Potential Map: Forest to Built-up land

#### 4.5 Model comparison and validation

The LCM predicted the LULC map of 2016 which was compared with the 2016 LULC map of reality (the ‘Hansen\_GFC-2016-v1.4\_last\_10N\_060W1’) as depicted in Figure 21. After performing the stratified random sampling technique with ArcMap 10.4, an error matrix was produced (Table 16) with the ERRMAT module in Idrisi. The output of the Errmat module resulted in a minimum overall accuracy of 84.20 % and a KIA of 0.7989, meaning that there is a rounded up 80 % good agreement between the real and predicted LULC map of 2016 than just by chance. The validity of the predicted map of 2016 was also assessed against the reference map of Hansen that depicts reality, through the VALIDATE module in Idrisi which measures the agreement between the two LULC maps of 2016, by comparing the entire maps, involving areas with no potential to change. The results of the module was a K-standard of 98.00%, meaning a very good or strong agreement between the reference and the predicted map of 2016. The K-no specifying quantity was 99.00%, meaning a very good or strong agreement between the two maps. The Kappa for location being a more useful criteria for validation according to Pontius (2000) was 99.00%, meaning a strong allocation agreement which is due to the optimal match of spatial allocation of the predicted LULC map of 2016.

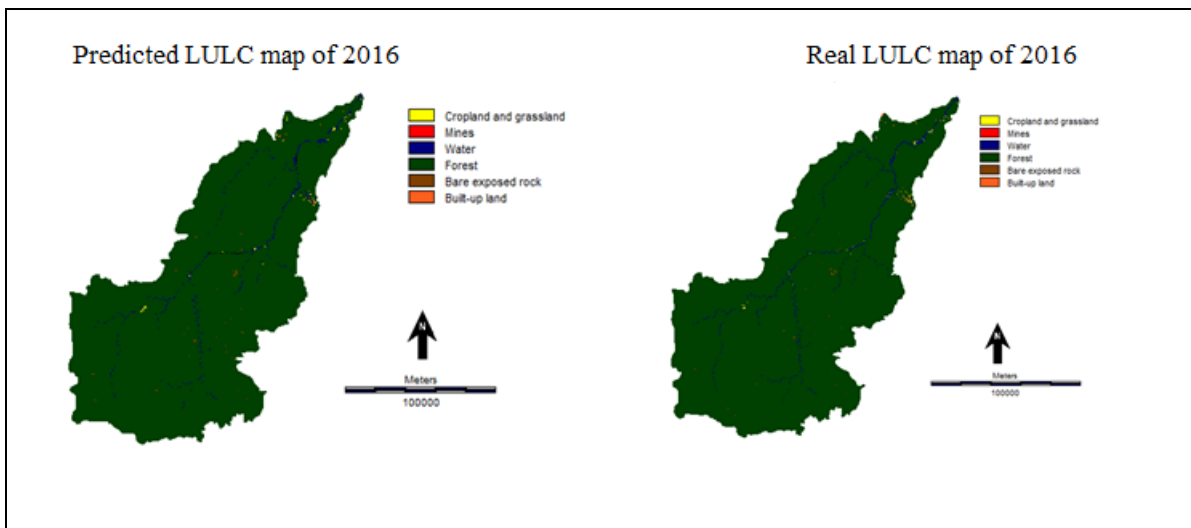


**Figure 21.** Comparison of the LULC map of reality Hansen\_GFC-2016-v1.4\_last\_10N\_060W1 vs. the Predicted land cover map of 2016

**Table 16:** Error Matrix for the Predicted LULC map of 2016

		Reference points 2016						
		Cropland and Grassland	Mines	Water	Forest	Bare exposed rock	Built-up land	Total
LULC map 2016	Cropland & Grassland	30	1	0	15	0	1	47
	Mines	1	41	0	0	0	1	43
	Water	2	2	48	0	0	1	53
	Forest	1	1	2	100	2	1	107
	Bare exposed rock	0	0	0	4	44	0	48
	Built-up land	2	5	0	13	0	30	50
	Total	36	50	50	132	46	34	348

#### 4.6 Change prediction

The trend of the predicted quantity of changed area over time, is illustrated in line graphs in Figure 22 and Figure 23. In Figure 22, it can be seen that the lines in the graphs for both Forest area and Cropland and Grassland are fairly smooth, while the trend of the lines for Built-up land and Mines went up gradually. In Figure 23, it can be seen that the gradient of the lines changes relatively for the predicted area for Forest, showing a downward trend and an upward trend for Built-up land and Grassland and Cropland, while the trend from ‘Forest to Mines’ goes up till 2020 and remained constant till 2040. Table 17 and Table 18 represent changed area in km<sup>2</sup> for respectively scenario1 and scenario 2. A relative slighter decrease in Forest area can be seen for scenario 2 compared to scenario 1. The largest change in area can be notice from ‘Forest to Cropland and Grassland’ for the predicted years of scenario 1 and 2, while the predicted quantity of change remained the same for the year 2040. Obviously the predicted quantity of change remained the same for 2030 and 2040 from ‘Forest to Mines’ for scenario 2 , while the predicted quantity of change increased slightly from ‘Forest to Built-up’ land till year 2030 and remained constant till 2040.

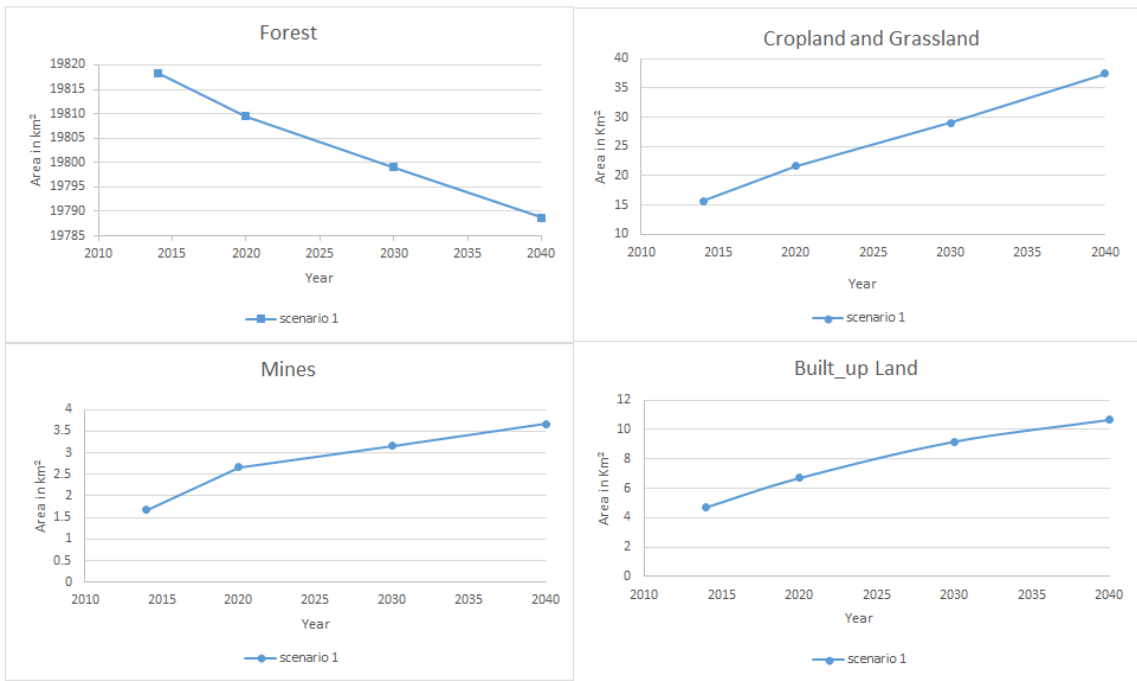


**Figure 22.** The trend of classes changing in area size (km<sup>2</sup>) for scenario 1.

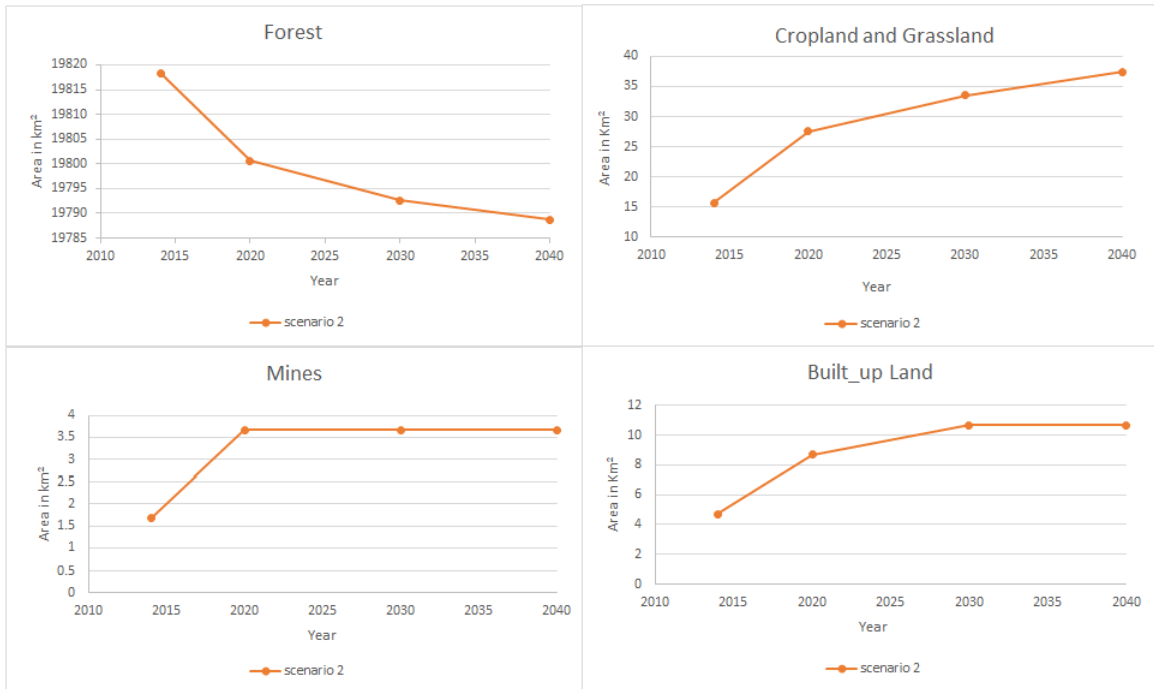


**Figure 23.** The trend of classes changing in area size (km<sup>2</sup>) for scenario 2.

**Table 17.** Changes in areas of LULC classes of interest under scenario 1 for the year 2014, 2020, 2030 and 2040.

	Area (km <sup>2</sup> )	Changed Area (km <sup>2</sup> ) under scenario 1					
	2014	2020	%/yr.	2030	%/yr.	2040	%/yr.
<b>Forest</b>	19818.38	-8.92	-0.01	-19.38	-0.006	-29.72	-0.006
<b>Cropland and Grassland</b>	15.68	5.95	5.42	13.38	10.90	21.8	8.85
<b>Mines</b>	1.68	0.99	8.42	1.48	11.01	1.98	8.09
<b>Built-up land</b>	4.71	1.98	6.01	4.46	11.45	5.94	8.37

**Table 18.** Changes in areas of LULC classes of interest under scenario 2 for the year 2014, 2020, 2030 and 2040.

	Area (km <sup>2</sup> )	Changed Area (km <sup>2</sup> ) under scenario 2					
	2014	2020	%/yr.	2030	%/yr.	2040	%/yr.
<b>Forest</b>	19818.38	-17.83	-0.01	-25.76	-0.008	-29.72	-0.006
<b>Cropland and Grassland</b>	15.68	11.89	10.83	17.84	12.58	21.8	8.85
<b>Mines</b>	1.68	1.98	16.84	1.98	12.82	1.98	8.09
<b>Built-up land</b>	4.71	3.96	12.01	5.94	13.30	5.94	8.37

It can be observed from Figure 24 that the result of scenario mapping for change predictions, namely the hard predicted LULC maps shows simulations of deforestation allocation such as increased patches of ‘Cropland and Grassland’, that can be observed along the river and creeks which was the largest change in area with the most potential to change followed by increased patches of ‘Built-up land’ near the Greenstone belt and little change from ‘Forest to Mines’ near the Mining areas. The soft prediction maps in Figure 25 show areas vulnerable to change. The portion of the study area overlapping with the Greenstone belt and gold mining exploration areas, shows the highest vulnerability to change, concentrating cells with higher deforestation risk. Cells with values close to 1 have high deforestation risk and cells with low deforestation risk have values to 0 (zero). This means that in the next years, it is highly probable that most of the deforestation at the Tapanahony River basin will occur in this region according to both scenarios. It was also found that the implementation of the proposed Tapajai roads slightly expands the vulnerability along the mid part of the Tapanahony River basin. The vulnerability also increased and spreads along the river at the vicinity of the community territories living in the southern part of the watershed.

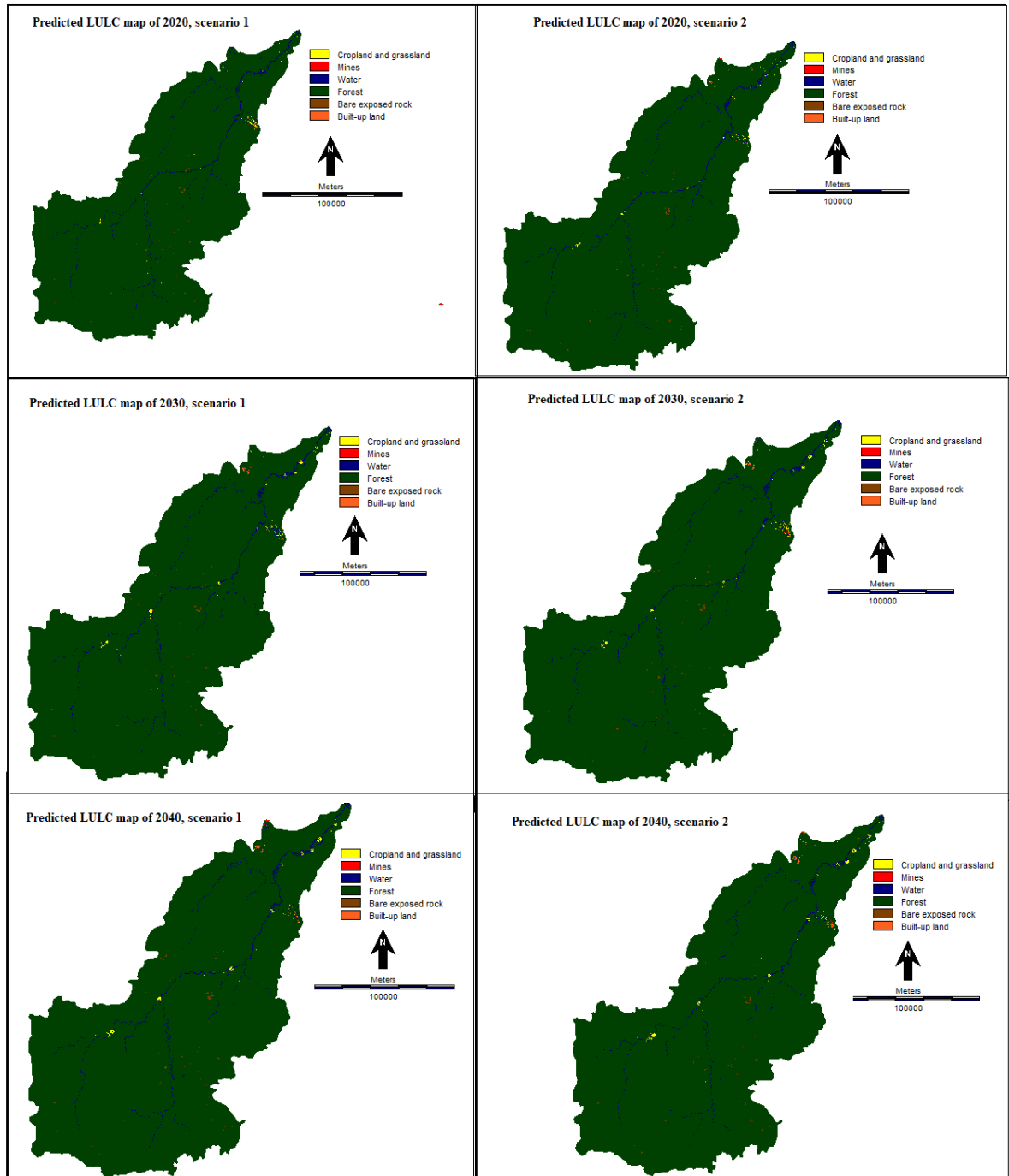


**Figure 24.** Hard predicted LULC maps of 2020, 2030 and 2040 for scenario 1 and scenario 2

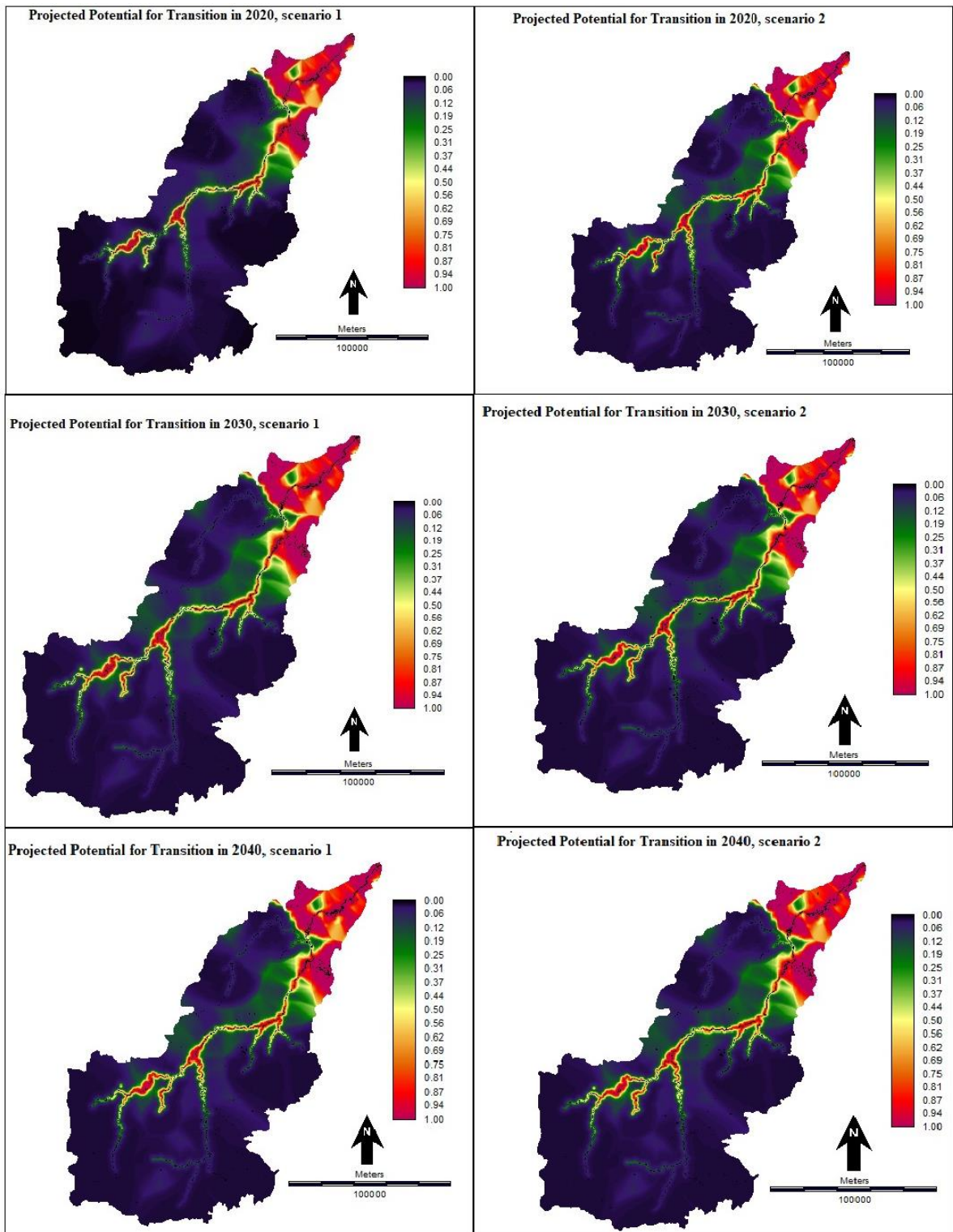


**Figure 25.** Soft predicted LULC maps of year 2020, 2030 and 2040 under scenario 1 and scenario 2

## 5 Discussion

The first objective of this study was to analyze and model the past LULC changes between 2004 and 2014, using remotely sensed data. Land-cover maps were created from Landsat 5 and Landsat 8 imagery. The overall accuracy rates and the KIA for both the classified images of the categorical maps of 2004 and 2014 were well above 80%, meaning a very good agreement. The capacity of identifying mining areas is more precise using high spatial resolution imagery for validation purposes when considering the omission and commission errors between water and alluvial gold mining points of the error matrix. Although several studies has found out for 'Mining' to be the main driver of deforestation in Suriname (Unique, 2017; FAO Forestry Department, 2010 a), the study area has historically a low deforestation rate, considering the results of the past LULC change analysis of 2004-2014 using the Markov method available in LCM. The overall main cause of deforestation between 2004 and 2014 within the study area, was the increase change from forest to 'Cropland and Grassland'.

The second objective of this study was to analyze the driving forces for deforestation. The driver variable affecting the transition from 'Forest to Mines' was the 'Distance to Mines' followed by 'Distance to Road', meaning the areas with the highest potential to change to Mines were located around the Mining areas itself situated in the gold exploration areas within the Greenstone belt. Unpaved roads emerge during mining activities, which in turn trigger interest to explore more mines and extraction activities. This is in agreement with other studies were infrastructure of existing mines gain access to areas with proven gold deposits (Crema, 2014; Unique, 2017). The driver variables most affecting the transition from 'Forest to Cropland and Grassland' were 'distance to rivers'. Shifting cultivation grounds are found scattered along the rivers or along creeks in the vicinity (within 5 km radius) of the villages and happens in cycles, not having a specific pattern (Amazon Conservation Team, 2010). 'Grassland' also appears mostly around built-up lands, settlements and mining activities, as they are a result of human activities. The most influential driver most affecting the transition from 'Forest to Built-up land' was 'distance to Greenstone belt' followed by 'distance to gold exploration'. Most of the villages, settlements and unpaved roads are concentrated within the Greenstone belt and gold exploration areas at the northern part of the Tapanahony River basin, were most of the Maroon communities live. These Maroon communities are facing commercial influence as a consequence of artisanal goldmining and make a living out of it (Heemskerk, 2000). The urge for prospecting and extracting gold causes 'Built-up land' to appear as they are a result of human activities.

Eastman (2012) acknowledges that a high Cramer V does not guarantee a good model. MLP results of the test and selection of drivers showed that even a lower Cramer V's (Table 12) for the transition from 'Forest to Mines', 'Forest to Built-up land' and from 'Forest to Cropland and Grassland', resulted to be the most influential variable for example 'distance to road', 'distance to greenstone-belt' and 'distance to gold exploration'. Clark labs recommends not using the test and selection of driver variables output, but using the useful html output after transition potential modeling as it did indicate that these drivers variables were affecting the transitions.

The third objective of this study was to predict the LULC changes for the years 2020, 2030 and 2040 under the business as usual and planning intervention scenarios. A model validation was done with the deforestation map of high temporal and spatial resolutions of Hansen et al. for the year 2016 to validate the LULC model. The Kappa statistics showed an overall accuracy of 84.20 % and a KIA of  $\pm 80\%$ , which is a good agreement between the reference and the predicted map of 2016 and indicates that the classified map is of good representation of reality. (Congalton, et al., 2008). The Kappa for location is a more useful criteria for validation according to Pontius (2000) and was 99.00%, meaning a strong allocation agreement which is due to the optimal match of spatial allocation of the predicted LULC map of 2016. The scenario mapping produced LULC hard and soft maps for the years 2020, 2030 and 2040. The LCM predicted a further slight decrease in Forest and a gradual increase in 'Cropland and Grassland', followed by a slight increase of changed areas in 'Built-up land' followed by 'Mines' for the business as usual scenario. The increase in land change area from 'Forest to Cropland and Grassland' was notable for both scenarios since it was the largest change related to the other classes of interest. The LCM predicts LULC changes by projecting the historical change pattern into the future (Eastman, 2012). The results from the LULC change analysis indicates that there are historically no significant changes in the study area, that in turn didn't visualized extraordinary or notable changes on the hard predicted maps. The impact of the proposed Tapajai roads was analyzed through planning intervention in the LCM. The proposed roads did not have a significant impact on the quantity of changed areas from 'Forest to Mines'. This is also evident when looking at the vulnerability of the soft predicted maps were no significant changes can be visualized under the planning intervention scenario 2. This can be presumed when considering that the 'Distance to road' was not the most influential driver for the transitions being modeled.

## 6 Conclusions and recommendations

### 6.1 Conclusions

The free of charge Landsat 5 and Landsat 8 images, have proven to be sufficient to monitor the main causes of deforestation through image classification within the Tapanahony River basin. The classification using level II classes, yielded accuracies and KIA's well above 80%. The overall major observed change between 2004 and 2014 was a forest loss of 7.09 km<sup>2</sup>, within the Tapanahony River basin. Part of the deforestation was due to 3.63 km<sup>2</sup> of forest area transitioning to 'Cropland and Grassland', a slight amount of 0.88 km<sup>2</sup> of forest area transitioning to 'Mines', and 2.58 km<sup>2</sup> of forest area transitioning to 'Built-up land'. These trend of changes caused by human activities, were projected into the future for scenario mapping and the LCM produced the predicted LULC maps for 2020, 2030 and 2040. Areas showing little change between 2004 and 2014 did not change much in the predictions. From 2014 till 2040 'Cropland and Grassland', 'Mines' and 'Built-up land' are expected to increase under the business as usual scenario from 2020 till 2040, while the proposed Tapajai roads scenario were found to have a significant impact on the quantity of change for 'Cropland and Grassland' from 2020 till 2040 were the trend of deforestation continues, while no predicted quantity of change for 'Mines' is observed from 2020 till 2040 as well for 'Built-up land' starting from 2030 till 2040. The proposed roads did however have an influence on the predicted locations of change when observing the vulnerability. The portion of the study area which corresponds with the Greenstone belt, showed the highest vulnerability to change.

The main driving force with the highest weight of evidence for the transition from 'Forest to Mines', was 'Distance to Mines'. According with the model result, the existed mines of 2004 will trigger new mining areas at the close vicinity to emerge. The modeled zones of influences, predicted for these new 'Mines' occur mainly at the north part of the Tapanahony River basin along the Toso and the Sela creek, within the Greenstone-belt and gold exploration area, where forest will be cut and cleared. These modeled zones are identified areas with the potential for further deforestation. For the transition from forest to 'Cropland and Grassland', the main driver variables with the highest weight of evidence was 'Distance to rivers'. The increase in 'Cropland and Grassland' will occur along the rivers or creeks, while 'Grassland' will appear mostly near Built-up land, settlements and mining activities. Shifting cultivation happens in cycles and has no specific pattern. This can explain why the model could not predict the exact location for the class 'Cropland'. The conversion forest to 'Built-up land', was impacted by the driving forces 'Distance to Greenstone belt' followed by 'Distance to gold exploration'.

The increase in 'Built-up land' will occur mostly near the Greenstone belt. 'Distance to roads' was not found to be the driver variable most affecting deforestation in the Tapanahony River basin between 2004 and 2014, which explain the little or no significant impact on the quantity of changes for the prediction under the propose Tapajai roads.

## **6.2 Recommendations**

The Tapanahony River basin with no proper road establishment and sparsely populated by Indigenous and tribal communities, has historically a low deforestation rate. This does not alter the fact that deforestation will not increase or take place in the future within the basin. There is a growing demand of gold exploitation in the Greenstone belt overlapping the study-area. Gold deposits are abundant in the upper river basins of the Marowijne River (Tapanahony and Lawa) and tribal communities living along those rivers, have a long tradition in small scale gold operations. The presence of ASGM being informal due to the nature of alluvial deposits and weak state presence or control by the government in the interior can lead to further deforestation and deterioration of the ecosystem within the Tapanahony River basin. A similar study should be done, using high spatial resolution imagery and cloud-free data, in order to increase the capacity of identifying alluvial gold mining areas and achieve more accurate classification results in the case of national or international policy initiatives by means of investigating more classes of interest in the future. More accurate classification maps can lead to more accurate LULC change analysis and better assessments of the transition rate for the predictions.

The Tapajai project will provide increase electrical generation and improved supply reliability for the entire country and therefore is of national importance considering the economic competitiveness of the country. This on the other hand may expose the region to environmental change because this road will cut off through well preserved-environmentally sensitive areas of Tropical Rain Forest with high biodiversity and high availability of water resources, high ecologically and high cultural assets. Moreover, the area along the road have high socio-economic value, with rich areas of forestry resources and large reserves of gold. In this study, areas with the potential for further deforestation or high-risk areas have been identified and can be used as a baseline for further monitoring or comparing the deforestation of Tapanahony River basin for future purposes such as planning interventions.

In this research, drivers in a broad sense is reflecting both proximate and underlying causes, however it is important to address them separately and examine them at various scales for specific analysis and intervention strategies. Further causes of deforestation within the basin

should be investigated for example deforestation will increase in response to the French repressive policy against illegal- gold mining, making the mining areas susceptible by the movement of gold miners through the French Guiana border. This will lead to the expansion of illegal ASGM, further impacting the ecological conditions of the water basin (de Theije, 2015). Multidisciplinary study can be recommended to systematically assess underlying drivers and their relationship to and impact on proximate drivers. This will provide policy makers with inputs to implement measures to guide sustainable mining practices, the expansion of zoning within mining regions, active border cooperation with Suriname and neighbor countries and the elaboration of new legislation and regulations. These inputs will limit the uncontrolled expansion of informal or illegal goldmining in the future in order to protect the ecological integrity of the river basin, its waterways and ensure sustainable livelihoods to local populations.

A study can also be done regarding the effects of deforestation on the ecosystem services within identified high-risk or vulnerable areas. An economic evaluation of these ecosystem services could help promote forest conservation measures. Identified high-risk areas of deforestation and forest degradation can also be used in the REDD+ project panel offered by the LCM of the Idrisi software, where carbon emissions can be calculated in the historical period, under the business-as-usual scenario, and under future REDD+ scenarios.

The LCM was not able to predict the phenomenon of shifting cultivation accurately. Different modeling software such as the more complex LCM software programs Dinamica Ego or ClueScanner could be used to model the transition more accurately, predict the changes within this study area, delivering dynamic models that illustrates the potential impact of policy interventions in order to maximize ecosystem services.

## References

Amazon Conservation Team Suriname, 2010. Support for the sustainable development of the interior collective rights and land rights, tenure and use of indigenous peoples and maroons in Suriname final report. Support for the sustainable development of the interior –collective rights. Paramaribo, Suriname.

Algemeen Bureau voor de Statistiek. (2016). Milieu Statistieken Publicatie. Paramaribo, Suriname: Algemeen Bureau voor de Statistiek.

Anderson, J.R., et al. (1976). A Land Use and Land Cover Classification System for use with Remote Sensor Data. Geological Survey Professional Paper 964. United States Government Printing Office, Washington DC, USA

Atkinson, P.M. et al. (1997). Neural networks in remote sensing. *International Journal of Remote Sensing*, 18(4), 699-709.

Boksteen, L.W. Ir. (2009). Strategische analyse en participatief actieplan voor Zuid Oost Suriname. Deelstudie impact vergroting beschikbare hoeveelheid water in het bestaande Brokopondo Stuwmeer. Paramaribo, Suriname.

Campbell, J. (2006). *Introduction to remote sensing*, 7th edition, Taylor & Francis, London, England.

Congalton R.G., Green K., (2009). *Assessing the Accuracy of remotely Sensed Data-Principles and Practices*. Second edition, 183 pp. CRC Press, Taylor and Francis Group, Boca Raton, Florida

Coulter L., et al. (2016). Classification and assessment of land cover and land use change in Southern Ghana using dense stacks of Landsat 7 ETM+ imagery. *Remote Sensing of Environment* 184. Page 396-409.

Crabbe, S. and Djodjodikromo, M. (2012). *ACTO-Project: Monitoring Deforestation, Logging, and Land Use Change in the Pan Amazonian forests*. Paramaribo, Suriname

Crema, S. (2014). The regional scenarios modeling project for the Guiana Shield. Clark Labs-Clark University, USA.

Eastman, J.R. (2012). IDRISI Selva Manual Version 17. Clark Labs, Worcester, USA.

Elkhrachy, I. (2017). Vertical accuracy assessment for SRTM and ASTER Digital Elevation Models: A case study of Najran city, Saudi Arabia. *Ain Shams Engineering Journal*, Faculty of Engineering-Civil Department, Al-Azhar University, Cairo, Egypt.

Engebretson C. (2018). Landsat Thematic Mapper (TM) level 1 (L1). Data format control book (DFCB). U.S. Geological Survey.

Environmental Research Management (2011). Technical Proposal, Tapajai Hydropower Project Phase I. Staatsolie Maatschappij Suriname N.V.

Favero A., Sohngen B., Yuhan H., Jin Y. (2018). Global cost estimates of forest climate mitigation with albedo: a new integrative policy approach. *Environmental research letters* 13 (2018) 125002.

Foley, J. A., De Fries, R., Asner, G. P., Barford, C., Bonan, G., Carpenter, S. R., Gibbs, H. K. (2005). Global consequences of land-use. *Science*, 309(5734), 570–574.

Fonseca, G. A. B. da, Rodriguez, C. M., Midgley, G., Busch, J., Hannah, L., & Mittermeier, R. A. (2007). No Forest Left Behind. *PLOS Biology*, Vol. 5, 8, pp. 1645-1646.

Food and Agriculture Organization of the United Nations (2007). Definitional issues related to reducing emissions from deforestation in developing countries. *Forests and Climate Change Working Paper 5*. Rome, Italy.

Food and Agriculture Organization of the United Nations. (2015). *Global Forest Resources Assessment 2015, How are the world's forests changing? Second edition*. Rome, Italy.

Forestry Department Food and Agriculture Organization of the United Nations (2010 a). *Global Forest Resource Assessment 2010, Country Report Suriname*. Rome, Italy.

Forestry Department Food and Agriculture Organization of the United Nations (2010 b) Global Forest Resource Assessment 2010. Forest Resources Assessment Program, Working paper 144/E Rome 2010. Rome, Italy.

Fung-Loy, K. (2014). Analysis and modeling of land use and land cover change in the Upper-Suriname River basin. Anton de Kom University of Suriname. Paramaribo, Suriname.

Geist, H. & Lambin, E., 2002. Proximate Causes and Underlying Driving Forces of Tropical Deforestation. *BioScience*, 52(2):143-150

GONINI, (2018). GONINI National Land Monitoring System of Suriname. [Online] <http://www.gonini.org/>.

Hansen, M. C., et al. (2016). High-Resolution Global Maps of 21st-Century Forest Cover Change. *Science* 342. [Online]. [http://earthenginepartners.appspot.com/science-2016-global-forest/download\\_v1.4.html](http://earthenginepartners.appspot.com/science-2016-global-forest/download_v1.4.html). University of Maryland. Department of Geographical Sciences.

He, C., Okada, N., Zhang, Q., Shi, P., & Zhang, J. (2006). Modeling urban expansion scenarios by coupling cellular automata model and system dynamic model in Beijing, China. *Applied Geography*, 26(3–4), 323–345.

Heemskerk, M. (2000). Driving forces of small-scale gold mining among the Ndjuka Maroons: a cross scale socioeconomic analysis of participation in gold mining in Suriname. PhD dissertation, Department of Anthropology. Florida, USA.

Heemskerk, M., et al. (2007). Trio Baseline Study. A sustainable livelihoods perspective on the Trio Indigenous Peoples of South Suriname. Amazon Conservation Team Suriname. Paramaribo, Suriname.

Hubert-Moy, L., Cotonnec, A., Le Du, L., Chardin, A. & Perez, P. (2001). ‘A Comparison of Parametric Classification Procedures of Remotely Sensed Data Applied on Different Landscape Units’, *Remote Sensing of Environment*, Vol. 75, pp. 174-187.

Huiran Han, Chengfeng Yang and Jinping Song. (2015). Scenario Simulation and the Prediction of Land Use and Land Cover Change in Beijing, China. *Sustainability*. 2015, pp 4260-4263.

Jain, R.K., et al. (2017). Modeling Urban Land Cover Growth Dynamics Based on Land Change Modeler (LCM) Using Remote Sensing: A Case Study of Gurgaon, India. *Advances in Computational Sciences and Technology*. Vol. 10, pp. 2947-2961.

Jiang Zying. (2007). The road extension model in the land change modeler for ecological sustainability of IDRISI. Graduate School of Geography, Clark University, USA.

Kamusoko, C., Aniya, M., Adi, B., & Manjoro, M. (2009). Rural sustainability under threat in Zimbabwe-Simulation of future land use/cover changes in the Bindura district based on the Markov-cellular automata model. *Applied Geography*, 29 (3), 435- 447.

Kinoti Kibetu, (2017). Monitoring Nature of Nairobi City Land Features from Landsat 5 Images Using Index-Based Mapping. Vol.1. Department of Social Sciences, Chuka University, Chuka, Kenya

Kissinger, G. et al. (2012). Drivers of Deforestation and Forest Degradation. A Synthesis Report for REDD+ Policymakers. Vancouver, Canada.

Li, X., & Yeh, A. G.-O. (2002). Neural-network-based cellular automata for simulating multiple land-use changes using GIS. *International Journal of Geographical Information Science*, 16(4), 323–343.

Leh, M., Bajwa, S. and Chaubey, L. (2013). Impact of land use change on erosion risk: an integrated remote sensing, geographic information system, and modeling methodology. *Land Degradation & Development*. 2013, Vol. 24, 5, pp. 409–421.

Lillesand, M. et al. (2015). *Remote sensing and image interpretation*, seventh edition. John Wiley & Sons. USA.

Lu, D., Weng, Q., (2007). A survey of image classification methods and techniques for improving classification performance, *International Journal of Remote Sensing*, Vol. 28, pp. 823-870.

Mas, Jean-François, (2014). Inductive pattern-based land use/cover change models: A comparison of four software packages. *Environmental Modelling & Software*. Vol. 51, pp. 94-111.

Millennium Ecosystem Assessment. (2005). *Ecosystems and Human Well-being: Synthesis*. Island Press, Washington, DC.

Mozumder, C., Tripathi, N. K., & Losiri, C. (2016). Comparing three transition potential models: A case study of built-up transitions in North-East India. *Computers, Environment and Urban Systems*, 59, 38–49.

Myburg, G. & Van Niekerk, A. (2013). Effect of feature dimensionality on object-based land cover classification: A comparison of three classifiers, *South African Journal of Geomatics*, Vol 2(1), pp. 13-27.

Myint, Soe W. and Okin, Gregory S. (2010). *Modeling Land-Cover Types Using Multiple Endmember Spectral Mixture Analysis in a Desert City*. University of California, Working Paper Number 2010 - 06

Nurmohamed, R., Donk, P. (2013). Development of digital elevation models for hydrologic modeling purposes for large river basins in Suriname. *Academic Journal of Suriname*, pp. 339-346. Paramaribo, Suriname.

Noordam, D., et al. (2007). *Wayana Baseline Study, A sustainable livelihoods perspective on the Wayana Indigenous Peoples living in and around Puleowime (Apetina), Palumeu, and Kawemhakan (Anapaike) in Southeast Suriname*. Amazon Conservation Team Suriname, Final Report, 2007. Paramaribo, Suriname.

OpenStreetMap, (2018). [Online], [http// www.openstreetmap.org/](http://www.openstreetmap.org/).

Policy Development Plan 2017-2021. Government of the Republic of Suriname Publication of the Stichting Planbureau Suriname (Suriname Planning Bureau Foundation).Paramaribo, Suriname.

Prieto-Amparan, J.A., et al. (2018). Atmospheric and Radiometric Correction Algorithms for the Multitemporal Assessment of Grasslands Productivity. Multidisciplinary Digital Publishing Institute Remote Sensing.

Rahm, M., et al. (2014). Monitoring the impact of gold mining on the forest cover and freshwater in the Guiana Shield. Study implemented in the framework of the REDD+ for the Guiana Shield project.

Ramirez-Gomez, S. (2011). Spatial Drivers of Deforestation in Suriname. Center for Agriculture research in Suriname, Tropenbos. Paramaribo,Suriname.

Regmi, R.R., Saha, S.K. and Balla, M.K. (2014). Geospatial Analysis of Land Use Land Cover Change Modeling at Phewa Lake Watershed of Nepal by Using Cellular Automata Markov Model. International Journal of Current Engineering and Technology. Vol. 4, No.1, pp. 260-267.

Roy, D.P., et al. (2014). Landsat-8: Science and product vision for terrestrial global change research. Remote Sensing of Environment 145, pp.254-172.

SBB, (2017). Technical report: Forest cover monitoring in Suriname using remote sensing techniques for the period 2000-2015. Paramaribo, Suriname.

SBB (Foundation for Forest Management and Production Control) 2018. Forest Reference Emission Level for Suriname's REDD+ Programme. Paramaribo, Suriname.

Sharma R., et al. 2017. High-Resolution Vegetation Mapping in Japan by Combining Sentinel-2 and Landsat 8 Based Multi-Temporal Datasets through Machine Learning and Cross-Validation Approach. Land. MDPI journals.

Soares-Filho, B. S., et al. (2002). DINAMICA – a stochastic cellular automata model designed to simulate the landscape dynamics in an Amazonian colonization frontier. *Ecological Modelling* 154(3): 217-235.

Staatsolie Maatschappij Suriname N.V. (2013). Environmental and Social Impact Assessment for Tapajai Hydropower Project Phase 1. Brokopondo, Suriname.

Stuckenberg, T., Münch, Z., van Niekerk, A. (2013). Multi-temporal Remote Sensing Land-cover Change Detection for Biodiversity Assessment in the Berg River Catchment. *South African Journal of Geomatics*. Vol. 2, 3, pp. 189-205.

Tadesse, H. and Falconer, A. (2014). Land cover classification and analysis using radar and Landsat data in North Central Ethiopia. Louisville: ASPRS 2014 Annual Conference.

Theije de, M. (2015). Small-scale gold mining and trans-frontier commerce on the lawa - river in and out of Suriname. *Language, Mobility and Identity*. E. B. Carlin, I lèglise, B. Migge and P. B. Tjon Sie Fat (Leiden: Brill) pp.58-75.

Unique, forestry and land use. (2016). Multi-Perspective Analysis of Drivers of Deforestation, Forest Degradation and Barriers to REDD+ Activities. Strengthening national capacities of Suriname for the elaboration of the national REDD+ strategy and the design of its implementation framework. Paramaribo, Suriname.

USGS.2018a USGS Global Visualization Viewer. USGS Global Visualization Viewer. [Online] U.S. Geological Survey. <http://earthexplorer.usgs.gov>

—. 2018b. USGS Global Visualization Viewer. *USGS Global Visualization Viewer*. [Online] U.S. Geological Survey. [https://topotools.cr.usgs.gov/GMTED\\_viewer/viewer.htm](https://topotools.cr.usgs.gov/GMTED_viewer/viewer.htm)

—. 2018c. USGS Global Visualization Viewer. USGS Global Visualization Viewer. [Online] U.S. Geological Survey. <https://lta.cr.usgs.gov/GMTED2010/>.

Van Dijck, P., et al. (2013). Handleiding bij seminars en trainingen over planning en beleid voor optimal landgebruik in het kader van grootschalige infrastructurele werken in Suriname, 2013. CEDLA, WWF .Amsterdam, The Netherlands.

Republic of Suriname, UNFCCC. (2015). Intended Nationally Determined Contribution under UNFCCC. Paramaribo, Suriname.

Souza-Filho, P., et al. (2018). Mapping Mining Areas in the Brazilian Amazon Using MSI/Sentinel-2 Imagery (2017). Remote Sensing Division, National Institute for Space Research (INPE), Av. dos Astronauta. Remote Sensing. MDPI, Basel, Zwitserland.

Tiwari, A., & Jain, K. (2014). GIS Steering smart future for smart Indian cities. International Journal of Scientific and Research Publications, 4(8), pp.442- 446.

Vanonckelen, S., et al. (2013). The effect of atmospheric and topographic correction methods on land cover classification accuracy. International Journal of Applied Earth Observation and Geoinformation 24 (2013) 9-21.

Warner, T.A., & Campagna, D.J. (2013). Remote Sensing with IDRISI A Beginner's Guide. Geocarto International Centre Ltd.

Watson P.F. and Petrie A., (2010). Method for agreement analysis: A review of correct methodology. Volume 73, Pages 1167-1179. London, United Kingdom.

Wilson, C. and Weng, Q. (2011). Simulating the impacts of future land use and climate changes on surface water quality in the Des Plaines River watershed, Chicago Metropolitan Statistical Area, Illinois. Science of the Total Environment. 409, pp. 4387–4405.

Yongnian Gao., et al. (2009). LULC Classification and Topographic Correction of Landsat-7 ETM+ Imagery in the Yangjia River Watershed: the Influence of DEM Resolution. International Institute for Earth System Science (ESSI), Nanjing University. Nanjing 210093, P.R. China.

Zhang, Z., et al. (2014). Integration of Satellite Imagery, Topography and Human Disturbance Factors Based on Canonical Correspondence Analysis Ordination for Mountain Vegetation Mapping: A Case Study in Yunnan, China. *Remote Sensing*. Vol. 6, 2, pp. 1026-1056.

Zhang, C., et al. (2010). Simulation of land use spatial pattern of towns and villages based on CA–Markov model. Beijing China. *Mathematical and Computer Modelling*. Vol. 54, pp. 938–943.

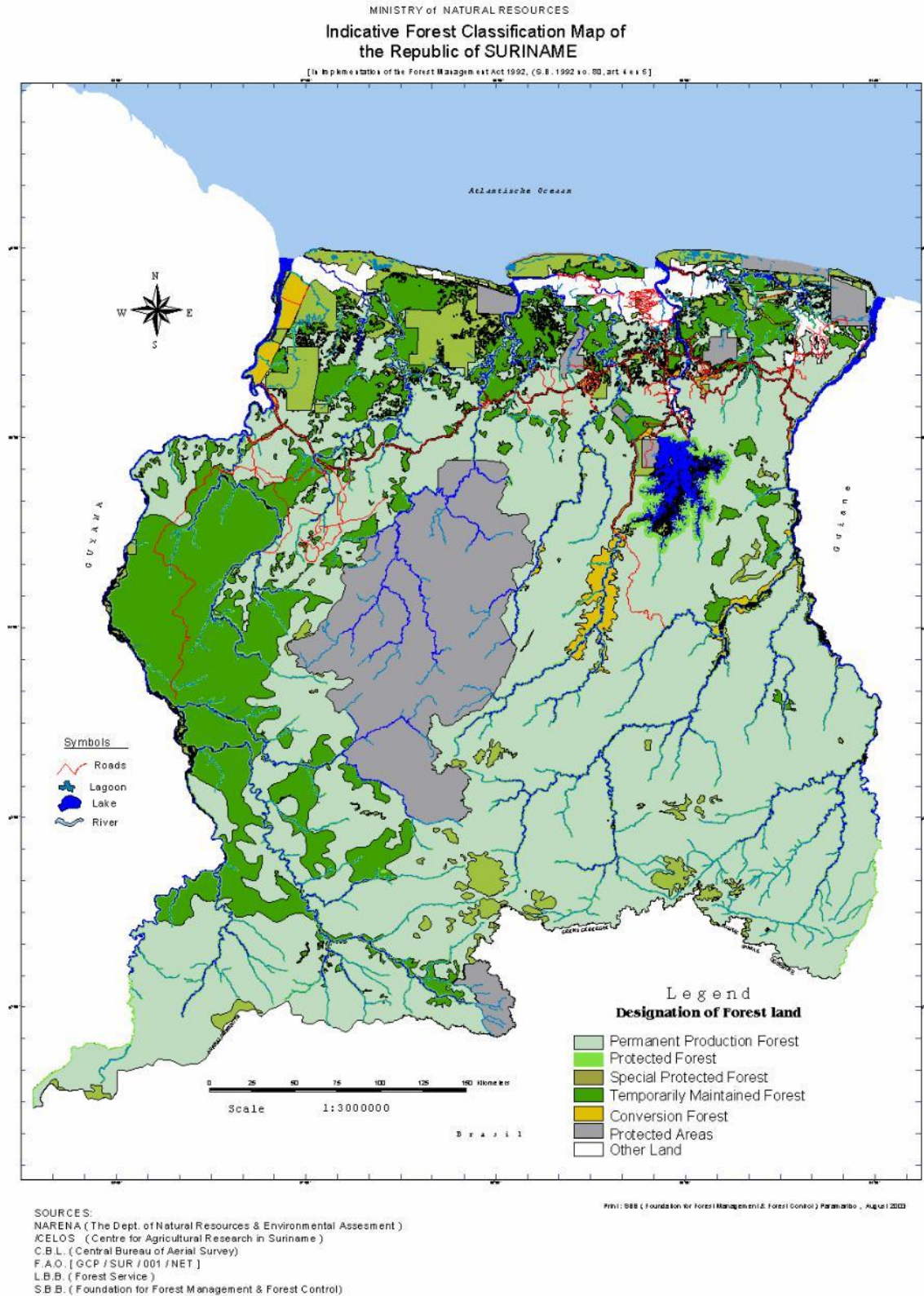
Zhu, Z., et al. (2018). Cloud and Cloud Shadow Detection for Landsat Images: The Fundamental Basis for Analyzing Landsat Time Series. *Global Environmental Remote Sensing*. University of Connecticut.

# Appendices

## Appendix 1. USGS land use and land cover classification system

<b>II</b>	<b>Level II</b>
1. Urban or built-up land	1.1 Residential
	1.2 Commercial and services
	1.3 Industrial
	1.4 Transportation, communications and utilities
	1.5 Industrial and commercial complexes
	1.6 Mixed urban or built-up land
	1.7 Other urban or built-up land
2. Agricultural land	2.1 Cropland and pasture
	2.2 Orchards, groves, vineyards, nurseries and ornamental horticultural areas
	2.3 Confined feeding operations
	2.4 Other agricultural land
3. Rangeland	3.1 Herbaceous rangeland
	3.2 Shrub and brush rangeland
	3.3 Mixed rangeland
4. Forest land	4.1 Deciduous forest land
	4.2 Evergreen forest land
	4.3 Mixed forest land
5. Water	5.1 Streams and canals
	5.2 Reservoirs
	5.3 Reservoirs
	5.4 Bays and estuaries
6. Wetland	6.1 Forested wetland
	6.2 Non forested wetland
7. Barren land	7.1 Dry salt flats
	7.2 Beaches
	7.3 Sandy areas other than beaches
	7.4 Bare exposed rock
	7.5 Strip mines, quarries and gravel pits
	7.6 Transitional areas
	7.7 Mixed barren land
8. Tundra	8.1 Shrub and herbaceous tundra
	8.2 Herbaceous tundra
	8.3 Bare ground tundra
	8.4 Wet tundra
	8.5 Mixed tundra
9. Perennial snow or ice	9.1 Perennial snowfields
	9.2 Glaciers

## Appendix 2. Indicative Classification Map of the Republic of Suriname



### Appendix 3. Error matrix of the landsat 2004 classification map

		Reference points 2004							Error Commission
		Cropland & Grassland	Mines	Water	Forest	Bare exposed rock	Built- up land	Total	
2004	Cropland & Grassland	48	0	0	3	0	2	53	0.0943
	Mines	0	6	0	1	0	0	7	0.1429
	Water	1	0	44	5	0	0	50	0.1200
	Forest	1	2	2	128	1	9	143	0.1049
	Bare exposed rock	0	0	1	2	45	0	48	0.0625
	Built-up land	0	4	0	0	0	45	49	0.0816
	<b>Total</b>	50	12	47	139	46	56	<b>350</b>	
Error of Omission		0.0400	0.5000	0.0638	0.0791	0.0217	0.1964		